https://www.osti.gov/pages/servlets/purl/1365805
Solar Energy xxx (2017) xxx–xxx

SAND2017-6158J

Contents lists available at ScienceDirect

Solar Energy

journal homepage: www.elsevier.com/locate/solener

Advances in central receivers for concentrating solar applications

Clifford K. Ho

Sandia National Laboratories, United States

ARTICLE INFO

Article history:
Received 16 January 2017
Received in revised form 10 March 2017
Accepted 15 March 2017
Available online xxxx

Keywords:
Central receivers
Concentrating solar
Particle receivers
High temperature receivers

ABSTRACT

This paper provides a review of current state-of-the-art commercial central receiver systems and emerging technologies intended to increase the outlet temperature to >700 °C. Research on particle-based, gas-based, and liquid-based receiver designs that can achieve these higher temperatures are discussed. Particle-based technologies include directly irradiated designs (free-falling, obstructed, centrifugal) and enclosed designs (gravity fed, fluidized). New gas-based receivers include micro-channel designs and light-trapping configurations that increase the surface area, heat transfer, and solar absorptance to enable higher fluxes and pressures. Liquid-based receivers and materials that are reviewed include high-temperature halide salts (chlorides and fluorides), carbonate salts, and liquid metals (sodium and lead bismuth). Advantages and challenges associated with each of the technologies and receiver designs are presented.

1. Introduction

Central receivers have been researched and developed for concentrating solar power (CSP) applications since the 1970s. The use of central receivers for CSP enables greater solar concentrations and overall efficiencies than line-focus systems like parabolic troughs, and central receivers can employ thermal storage more readily than distributed point-focus technologies like dish engines.

Central receivers have used liquid (e.g., water, molten salt), gas (e.g., air), and solid media (e.g., ceramic particles) as the heat-transfer and/or storage media. Liquid-based receivers typically use panels of tubes that are irradiated by concentrated sunlight and cooled by the flowing fluid. The panels of tubes can be contained inside a cavity receiver or arranged in a cylindrical or cubical configuration. Cavity receivers may reduce radiative and convective heat losses relative to external receiver designs, and the annual optical efficiency of a north-facing receiver (in the northern hemisphere) or south-facing receiver (in the southern hemisphere) is typically greater (by 10% or more) than an external receiver design with a surround heliostat field (Falcone, 1986). However, cavity receivers require taller towers to "see" all of the heliostats in a north or south heliostat field relative to a surround field for a given power requirement. Water and direct-steam central receivers have been deployed commercially and have the benefit of avoiding exergy losses and expenses associated with heat exchangers between the receiver and the power block. However, storage of the high-pressure steam is difficult. Molten-salt can be stored readily and heated to high temperatures (up to ~600 °C for nitrate salts) (Bradshaw and Meeker, 1990), but trace heating is required throughout the system to prevent freezing of the molten salt, which occurs at temperatures up to ~200 °C.

Gas receivers can use tubes or volumetric honeycombs and channels to heat air or other gases to high temperatures for Brayton power cycles or to heat a storage media (e.g., solid particles, concrete, graphite, phase-change material). Tubular receivers employ a closed-loop system that pumps gas, often at high pressures over 100 bar, through the irradiated tubes. Heat transfer limitations from the tube walls to the gas is a significant challenge. Volumetric receivers typically use an open-loop system with air as the heat-transfer fluid. Air is drawn through channels or honeycomb blocks that are irradiated by the concentrated sunlight. The air is heated as it flows through the irradiated structure, which ideally allows light to penetrate deep into the receiver so that the hottest part is in the interior, away from the aperture. However, most studies have shown that the aperture of the volumetric receiver is the hottest portion, yielding significant radiative losses to the environment.

Particle-based receivers use small solid particles that are heated by concentrated sunlight. The particles can be heated to temperatures above 1000 °C, stored, and used for process heat or electricity production. A significant advantage of particle receivers is that the particles can be irradiated directly, eliminating heat-transfer resistance and flux limitations associated with indirect heating through tube walls.

E-mail address: ckho@sandia.gov

http://dx.doi.org/10.1016/j.solener.2017.03.048
0038-092X/

1.1. Historical overview

Fig. 1 shows a timeline of significant receiver developments and associated CSP events since the 1970s. In 1978, the first central receiver test facility was built at Sandia National Laboratories in Albuquerque, NM. The facility includes a 61-m-tall tower with over 200 heliostats (each 37 m^2) in the north field for testing various receiver designs and materials. In the 1980s and 1990s, the first pilot-scale central receiver power tower systems using direct-steam (Solar One) and molten-salt (Solar Two) receivers were demonstrated in Daggett, CA, with a capacity of 10 MW_e. The first commercial parabolic trough plants were built in the 1980s in southern California and are still operational today. In 2007–2009, the first commercial power tower plants were built near Seville, Spain, and consisted of a 10 MW_e and 20 MW_e saturated-steam central receiver systems. In 2010, a 1.5 MW_e commercial dish/engine plant was constructed in Arizona (but went bankrupt a year later). In 2011, the first commercial molten-salt power-tower plant, Gemasolar, was built near Seville, Spain. Also in 2011, the U.S. Department of Energy initiated the SunShot program to bring unsubsidized costs of solar energy down to $0.06/kW h to be competitive with fossil fuels. In 2014, three large superheated-steam receivers were built at Ivanpah, CA, with a gross capacity of 390 MW_e. In 2015, a 110 MW_e molten-salt power tower was built in Tonopah, NV. Additional details of these commercial systems are provided in subsequent sections.

1.2. The push toward higher receiver temperatures

Current commercial central receiver systems operate at temperatures below 600 °C. Increased operating temperatures of central receivers are currently being pursued to increase the thermal-to-electric efficiency of the power cycle. However, increased operating temperatures also increase radiative and convective heat losses of the receiver. As the receiver temperature increases, the solar-to-thermal efficiency, η_{th}, decreases while the thermal-to-electric efficiency, η_e, of the power cycle increases according to Carnot's theorem. The solar-to-thermal and thermal-to-electric efficiencies can be expressed as follows:

$$\eta_{th} = \frac{\alpha Q_{in} - Q_{loss}}{Q_{in}} = \alpha - \frac{\varepsilon\sigma T_R^4 + h(T_R - T_{amb})}{\eta_{field} E_{DNI} C} \quad (1)$$

$$\eta_e = 0.7\eta_{carnot} = 0.7\left(1 - \frac{T_c}{T_h}\right) \quad (2)$$

where Q_{in} is the irradiance on the receiver (W/m^2), Q_{loss} is the total radiative and convective energy losses from the receiver (W/m^2), α is the receiver solar absorptance, ε is the receiver thermal emittance, σ is the Stefan-Boltzmann constant (5.67×10^{-8} W/m^2 K^4), T_R is the receiver surface temperature (K), h is the convective heat transfer coefficient (W/m^2-K), T_{amb} is the ambient temperature (K), η_{field} is the heliostat field efficiency (including cosine losses, reflectance losses, and spillage), E_{DNI} is the direct normal irradiance (W/m^2), C is the concentration ratio (collector aperture area divided by the receiver area), T_c is the temperature of the power-cycle cooling source (K), and T_h is the temperature of the power-cycle heating source (K). A factor of 0.7 is used in Eq. (2) to account for engineering inefficiencies relative to the Carnot cycle.

Fig. 2 (left) shows the solar-to-thermal and thermal-to-electric efficiencies as a function of temperature for different concentration ratios. The product of Eqs. (1) and (2) yields the combined efficiency (solar-to-electric) and is plotted in Fig. 2 as a function of temperature for different concentration ratios. As the temperature increases, the combined efficiency increases until the radiative and convective losses of the receiver outweigh the gains in the power-cycle efficiency, at which the combined efficiency begins to decrease. Thus, for a prescribed concentration ratio, there exists a temperature at which the combined solar-to-electric efficiency exhibits a maximum. Fig. 2 also shows that the combined efficiency can be increased by increasing the concentration ratio. Increasing the concentration ratio effectively adds the same amount of power to a smaller area, which reduces the footprint for radiative and convective heat losses.

Central receiver systems are capable of achieving concentration ratios up to several thousand suns, but the peak flux is often limited by the heat-transfer fluid and its ability to absorb heat from the irradiated walls of the receiver tubes to prevent overheating. Table 1 provides a summary of typical allowable peak fluxes and resulting outlet temperatures for different heat transfer fluids and media used in central receiver systems. Challenges include the need for materials, heat-transfer fluids, and processes that maximize solar absorptance and minimize heat losses while operating at these higher temperatures and fluxes. Central receiver systems also require high reliability over thousands of thermal cycles.

This paper first presents an overview of current state-of-the-art commercial central receiver systems, which include saturated and superheated direct-steam receivers and molten-salt receivers. Emerging technologies to achieve higher temperatures and efficiencies for central receivers are then presented, which include particle-based, gas-based, and liquid-based receivers that enable higher temperatures and/or higher efficiencies. Challenges associated with each of the technologies are presented.

2. Commercial central receiver CSP plants

Of the nearly 5 GW_e of operational CSP capacity around the world at the end of 2016, just over 600 MW_e (or 13%) of capacity was from central-receiver power-tower plants (Mehos et al., 2016). The rest was predominantly from parabolic trough plants. However, as researchers and developers seek to achieve higher efficiencies and lower costs through direct storage and higher temperatures, more and more central receiver technologies are being developed. Of the nearly 5 GW_e of CSP plants that were under construction or announced at the end of 2016, about 60% or nearly 3 GW_e were based on central-receiver power-tower technology. All new central receiver CSP plants were being constructed or planned outside of the United States – in China, Chile, South Africa, Israel, and Morocco. Early central-receiver plants were predominantly direct-steam receiver systems, but many newer plants employ molten-salt for storage.

2.1. Direct-steam receivers

In 2007 and 2009, the first commercial central-receiver CSP plants producing grid-connected electricity became operational in southern Spain. Planta Solar 10 (PS10) and Planta Solar 20 (PS20) utilize direct-steam central receivers producing saturated steam at ~250–300 °C, 45 bar, for a power cycle employing wet cooling with net turbine capacities of 11 MW_e and 20 MW_e, respectively (Fig. 3. Both plants use cavity receivers that house tubular panels to heat the water/steam, and both plants use pressurized-water thermal storage systems to provide up to an hour of storage capacity. PS10 and PS20 are expected to generate 23 and 48 GW h of electricity per year, respectively.

In 2014, the Ivanpah Solar Electric Generating System became operational in southern California. Ivanpah consists of three separate central-receiver CSP units, each considerably larger than PS10 and PS20, with a total net capacity of 377 MW_e (Fig. 4). Each unit produces superheated steam at ~540 °C, 160 bar, to drive an air-cooled steam Rankine power cycle at potentially higher

Please cite this article in press as: Ho, C.K. Advances in central receivers for concentrating solar applications. Sol. Energy (2017), http://dx.doi.org/10.1016/j.solener.2017.03.048

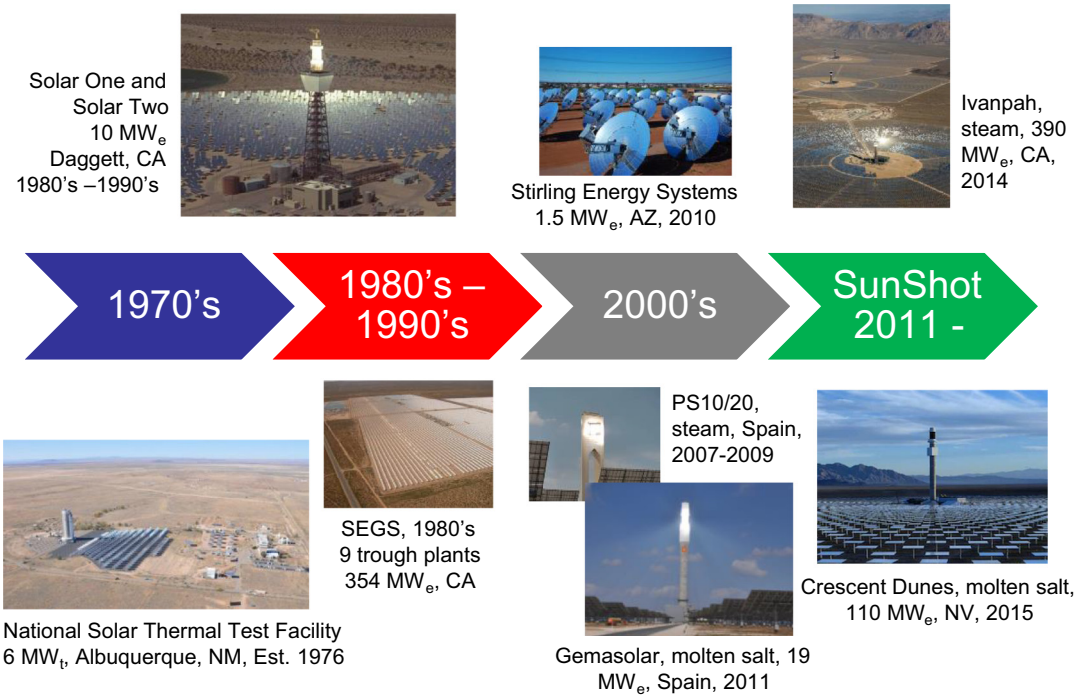

Fig. 1. Timeline of important events related to CSP and receiver development.

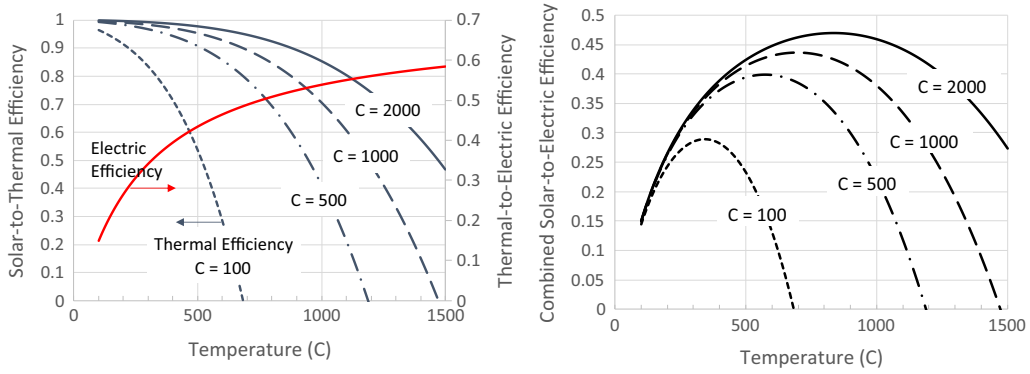

Fig. 2. Left: Plots of solar-to-thermal and thermal-to-electric efficiency. Right: Plot of solar-to-electric efficiency. ($\alpha = \varepsilon = 0.95$, $h = 10$ W/m^2-K, $\eta_{field} = 0.6$, $E_{DNI} = 800$ W/m^2, $T_{amb} = T_c = 20$ °C).

Table 1
Peak flux and outlet temperature for various heat transfer media used in central receiver systems. Adapted from Romero and González-Aguilar (2017).

Heat transfer media	Peak flux (kW/m^2)	Outlet temperature (°C)
Water/steam	~600	390–560
Molten nitrate salt	~1000	~600
Liquid sodium	~2500	~800
Volumetric air[a]	~1000	700–1000
Ceramic particles (direct heating)	~3000[b]	>1000

[a] Tubular air receivers require lower peak fluxes due to increased heat transfer resistance through tube walls.

[b] The peak flux for direct heating of ceramic particles will likely be limited by the receiver walls, insulation around the aperture, and/or accuracy of the heliostat field.

thermal-to-electric efficiencies than saturated-steam plants. The towers are 160 m tall, and the receivers are cubical in shape with sections to preheat, boil, and superheat the water/steam. The system is expected to generate over 1000 GW h of electricity annually.

Fig. 3. PS10 (left) and PS20 (right) near Seville, Spain – the world's first commercial central receiver (power tower) plants. Source: Wikipedia Commons.

Please cite this article in press as: Ho, C.K. Advances in central receivers for concentrating solar applications. Sol. Energy (2017), http://dx.doi.org/10.1016/j.solener.2017.03.048

Fig. 4. Images of the 377 MW_e Ivanpah Solar Electric Generating System. Source: C.K. Ho, Sandia National Laboratories.

In 2016, Khi Solar One began operations in South Africa and became the first power tower plant in Africa. Khi Solar One produces superheated steam for a 50 MW_e steam Rankine turbine and uses a natural updraft air-cooling condenser to reduce water use. Three cavity receivers situated atop a 205-m tall tower face south, east, and west to boil and superheat the steam to temperatures up to 530 °C at pressures of 120 bar (Fig. 5). The system has two hours of storage capacity using molten salt and is expected to generate 48 GW h of electricity annually.

2.2. Molten-salt receivers

Molten-salt receivers have the advantage of direct storage of the heat-transfer fluid, typically a mixture of potassium nitrate and sodium nitrate. Molten salt can be used between a wide temperature range (~200 °C to ~600 °C), which increases the volumetric storage capacity and reduces inventory and costs. However, heat exchangers must be used to extract the heat from the molten salt to generate steam (or heat another working fluid) for the power cycle.

2.2.1. Gemasolar

Gemasolar was the first commercial molten-salt central receiver plant that began operations in southern Spain in 2011. Gemasolar uses an external receiver on top of a 140 m tower to heat molten salt from 290 °C to 565 °C for a 20 MW_e steam-Rankine power plant. A two-tank direct-storage system provides 15 h of storage and 80 GW h per year (see Fig. 6).

2.2.2. Crescent dunes

In 2015, the Crescent Dunes Solar Energy Project in Tonopah, Nevada, became operational (Fig. 7). Crescent Dunes employs similar molten-salt receiver technology as Gemasolar, but it is significantly larger at a capacity of 110 MW_e. It is expected to produce 500 GW h per year. The 30-m-tall central receiver sits atop a 195 m tower and is irradiated by over 10,000 heliostats, each with 117 m^2 of reflective area. Each storage tank has a capacity of 13.6 million liters and is designed to hold 32 thousand metric tons of molten salt for 10 h of thermal storage. The hot molten salt is stored at 566 °C, and the "cold" salt is stored at 288 °C.

2.2.3. Molten-salt receivers in China

In 2016, two commercial 10 MW molten-salt central receiver systems were commissioned in China. The Supcon 10 MW molten-salt central receiver system became operational in August 2016 (the first molten-salt power tower in China), followed by the commissioning of the SunCan Dunhuang 10 MW molten-salt central receiver system in December 2016 with 15 h of thermal storage (Fig. 8). In September 2016, China announced a feed-in tariff of 1.15 RMB kW/h (~$0.17/kW h) for 20 new CSP power plants with a total capacity of 1.35 GW and a minimum of 4 h of thermal storage for each plant. The list includes 9 central receivers (685 MW), 7 parabolic troughs (464 Mw), and 4 linear Fresnel systems (200 MW).

Fig. 5. Khi Solar One direct-steam central receiver system in South Africa. Source: Wikipedia Commons.

2.3. Solid-based receivers

In 2011, a unique CSP plant with eight solar storage receivers composed of graphite blocks became operational. Each graphite block sits atop a tower with a face-down aperture that is illuminated by surrounding heliostats (Fig. 9). The graphite block is used to heat steam from 200 °C to 500 °C, which powers a 3 MW_e steam-Rankine cycle.

Particle-based receivers (e.g., falling, fluidized, centrifugal, enclosed) are also being investigated extensively, but commercial

Please cite this article in press as: Ho, C.K. Advances in central receivers for concentrating solar applications. Sol. Energy (2017), http://dx.doi.org/10.1016/j.solener.2017.03.048

Fig. 6. Gemasolar molten-salt power tower near Sevilla, Spain. Source: C.K. Ho, Sandia National Laboratories.

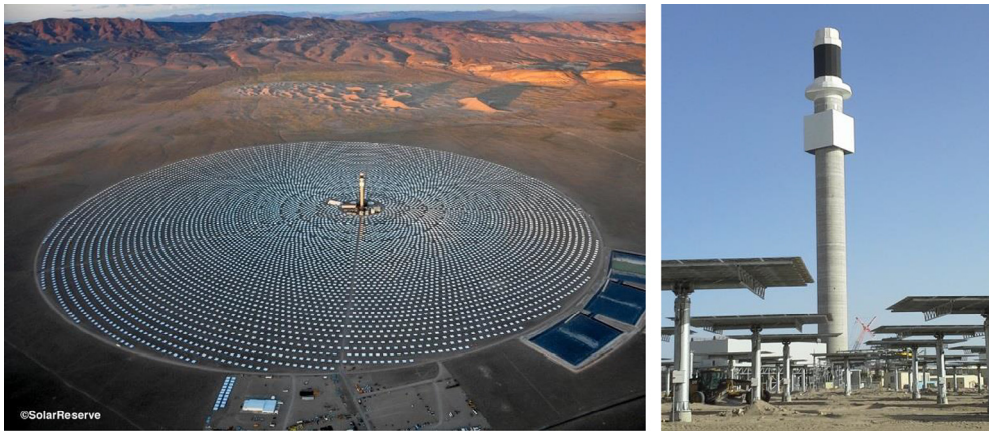

Fig. 7. Crescent Dunes Solar Energy Project in Tonopah, Nevada. (Sources: Left: SolarReserve. Right: C.K. Ho, Sandia National Laboratories).

Fig. 8. SunCan Dunhuang 10 MW molten-salt central receiver plant in China with 15 h of storage. Source: CSP Focus.

systems have not yet been deployed. In 2016, a demonstration project employing a modular 2 MW_t fluidized-bed particle receiver (STEM – Solar Thermo Electric Magaldi) became operational in Sicily. Concentrated sunlight illuminates a ground-based fluidized-bed receiver using beam-down optics from a surround heliostat field. The receiver heats steam up to 520 °C with up to 6 h of storage. Chirone et al. (2013) provide the technical basis and theory underlying this demonstration plant.

The following sections introduce some of the particle-based research, along with emerging gas-based and liquid-based central receiver technologies to accommodate higher temperatures (>700 °C).

Please cite this article in press as: Ho, C.K. Advances in central receivers for concentrating solar applications. Sol. Energy (2017), http://dx.doi.org/10.1016/j.solener.2017.03.048

Fig. 9. Solid-based (graphite) central-receiver system at Lake Cargelligo, NSW, Australia. Source: www.graphiteenergy.com.

3. Emerging technologies for central receivers

3.1. Particle-based receivers

This section reviews emerging particle-based technologies for central receiver systems.[1] A number of different particle heating methods have been studied and tested, including direct heating of the particles in free-falling, obstructed, centrifugal, and fluidized configurations, as well as indirect heating of the particles in enclosed configurations such as gravity-driven flow through tubes and fluidized particle flow in tubes and other enclosed receiver designs. A significant advantage of particle-based receiver systems relative to molten salts is the ability to operate over a wide range of temperatures. Particles can achieve high temperatures (>1000 °C) without decomposition or corrosion, and "low" temperatures (<200 °C) without the risk of freezing.

The following sections describe research on various particle receiver designs. While modeling of large-scale particle receivers has been performed, nearly all of the testing has been performed at the lab or pilot scales, ranging from ~0.1 to 1 MW_t. Scale-up of particle receivers to ~10 to 100 MW_t is necessary, and relevant design, performance, and cost parameters associated with large-scale particle receivers are discussed in Ho (2016).

3.1.1. Free-falling particle receivers

Free-falling particle receivers consist of particles falling through a cavity receiver, where the particles are irradiated directly by concentrated sunlight. The particles are released through an opening at the base of a hopper above the receiver, producing a thin sheet (or curtain) of particles falling through the receiver of varying patterns (Fig. 10). A slide gate or similar mechanisms can be used to control the mass flow of particles into the receiver to accommodate varying levels of irradiance and still achieve a desired particle outlet temperature. Previous studies have shown that for a given irradiance, higher particle mass flow rates reduce the particle outlet temperature due to increased particle shading, and vice versa (Ho et al., 2016a; Siegel et al., 2010).

A number of assessments and studies have been performed on direct free-falling particle receivers since its inception in the 1980s (Siegel et al., 2010; Hruby et al., 1984; Falcone et al., 1985; Hruby, 1986; Hruby and Steele, 1986; Evans et al., 1987; Meier, 1999; Chen et al., 2007; Klein et al., 2007; Kolb et al., 2007; Kim et al., 2010; Martin and John Vitko, 1982; Tan and Chen, 2010; Khalsa et al., 2011; Khalsa and Ho, 2011; Röger et al., 2011; Gobereit et al., 2012; Christian and Ho, 2013; Gobereit et al., 2013; Ho and Christian, 2013; Christian and Ho, 2014; Ho et al., 2014a; Ho et al., 2014b; Knott et al., 2014; Siegel et al., 2014; Ho et al., 2015; Siegel et al., 2015). In 2010, Tan et al. provided an overview of the prior research on free-falling particle receivers (Tan and Chen, 2010). The majority of those studies focused on modeling the particle hydraulics and radiant heat transfer to falling particles. Various geometries and configurations of falling particle receivers have been considered, including north/-south facing cavity receivers as well as face-down cavity receivers with a surrounding heliostat field (Gobereit et al., 2012; Gobereit et al., 2013; Röger et al., 2011). In 2008, Siegel et al. performed one of the first on-sun tests (in batch mode) of a simple free-falling particle receiver (Siegel et al., 2010; Ho et al., 2009). Those tests achieved ~50% thermal efficiency, and the maximum particle temperature increase was ~250 °C. More recently, Ho et al. (2016c) have performed on-sun tests of a 1 MW_{th} continuously recirculating particle receiver with bulk particle outlet temperatures reaching over 700 °C, and thermal efficiencies from ~50% to 80% (Ho et al., 2015, 2016b, 2017) (Fig. 11). Results showed that the particle temperature rise and thermal efficiency were dependent on particle mass flow rate and irradiance. The particle temperatures increased by 50–200 °C per meter of illuminated drop length for mass flow rates ranging from 1 to 7 kg/s per meter of particle-curtain width and for average irradiances up to ~700 kW/m^2. Higher particle mass flow rates yielded greater thermal efficiencies but lower particle temperature rise. As the particle mass flow rate increased (by increasing the particle discharge slot aperture size), the solids volume fraction increased and the particle curtain became more opaque. Thus, while more sunlight was intercepted and absorbed by the curtain for a greater thermal efficiency, additional shading and blocking reduced the bulk outlet temperature of the particles for a given irradiance. At higher irradiances of 1000 suns and higher, a greater amount of energy is absorbed by the particles for a given receiver size with relatively less heat loss than for lower irradiances. Technical challenges that were identified during the tests included non-uniform irradiance distributions on the particle curtain, variable mass flow rates, wind impacts, particle loss through the aperture, particle elevator reliability, and wear on the receiver walls from direct flux and high temperatures (>1000 °C).

The heat gain and exit temperature of particles falling through concentrated sunlight depends on the particle mass flow and amount of time spent in the heated region of the receiver. One way to increase the residence time is to recirculate the particles through the receiver multiple times, increasing in temperature over each successive drop. Previous studies have modeled recirculating particle flow through the receiver (Khalsa et al., 2011; Christian and Ho, 2013; Röger et al., 2011), and the recent on-sun testing by Ho et al. implemented a recirculating system (Ho et al., 2016c, 2017).

Kim et al. (2010) performed tests of particles free-falling along a 3 m drop length to evaluate the influence of wind direction (induced by fans). They found that the most particles were lost through the aperture when the wind was parallel to the aperture and when the cavity depth was shallow. The least amount of particle loss occurred when the wind was oriented directly toward (normal to) the aperture. Air recirculation and air curtains have been proposed as a means to mitigate the impacts of wind on particle flow and to reduce convective losses (Tan and Chen, 2010; Ho and Christian, 2013; Ho et al., 2014b; Kolb, 2012; Chen et al., 2009; Tan and Chen, 2009; Tan et al., 2009). Tan et al. (Tan and Chen, 2010, 2009; Chen et al., 2009; Tan et al., 2009) simulated the use

[1] Portions of Sections 3.1.1–3.1.5 have been reprinted with permission from Ho, C. K., 2016, A Review of High-Temperature Particle Receivers for Concentrating Solar Power, *Applied Thermal Engineering,* 109(Part B), p. 958–969.

Fig. 10. Free-falling particle curtains. Alternative release patterns have been investigated to increase light trapping (Ho et al., 2016b).

Fig. 11. On-sun testing of a falling particle receiver at the National Solar Thermal Test Facility at Sandia National Laboratories, Albuquerque, NM.

of an aerowindow (transparent gas stream along the aperture) to mitigate heat loss and wind impacts in falling particle receivers. Tan et al. (2009) found that aerowindows could reduce the heat loss by up to 10% depending on external wind direction and speed. However, no tests or validation studies were performed, and few parametric analyses have been conducted to evaluate important air-recirculation parameters. Ho et al. (2013, 2014b) performed experimental and numerical studies that evaluated the impact of an air curtain on the performance of a falling particle receiver. Unheated experimental studies were performed to evaluate the impact of various factors (particle size, particle mass flow rate, particle release location, air-curtain flow rate, and external wind) on particle flow, stability, and loss through the aperture. Numerical simulations were performed to evaluate the impact of an air curtain on the thermal efficiency of a falling particle receiver at different operating temperatures. Results showed that the air curtain reduced particle loss when particles were released near the aperture in the presence of external wind, but the presence of the air curtain did not generally improve the flow characteristics and loss of the particles for other scenarios. Larger particles and mass flow rates were also shown to reduce particle loss through the aperture. Numerical results showed that the presence of an air curtain could reduce the convective heat losses, but only at higher temperatures (>600 °C) when buoyant hot air leaving the aperture was significant.

3.1.2. Obstructed particle receivers

Another method to increase the residence time of particles within the concentrated sunlight is to obstruct the flow with porous structures or an array of obstacles that mechanically impede their descent and slow the downward velocity while still allowing direct absorption of concentrated solar energy. Early concepts of obstructed flow designs were introduced by Sandia in the 1980s by using ceramic structures suspended from the back wall to decelerate the particles (Hruby, 1986). No analytical or experimental studies were published, however. More recently, King Saud University and the Georgia Institute of Technology investigated the use of interconnected porous structures (metallic or ceramic foam blocks) to slow the flow of particles (Lee et al., 2015).

Additional studies evaluated the use of a staggered array of porous mesh structures (Ho et al., 2014a; Khayyat et al., 2015) to impede the flow of particles for increased residence time. In 2015, Ho et al. performed on-sun tests of a particle receiver consisting of a staggered array of stainless-steel chevron-shaped mesh structures (Ho et al., 2015, 2016c, 2017) (Fig. 12). Results showed that particle temperatures increased over 300 °C per meter of illuminated drop length for mass flow rates of 1–3 kg/s per meter of curtain width for irradiances up to ~1000 kW/m^2. Peak particle temperatures greater than 900 °C were achieved with bulk particle outlet temperatures reaching nearly 800 °C. While the obstructed-flow design seemed to improve the particle heating and reduce the impacts of wind and particle loss through the aperture, there were problems with the stainless steel 316 mesh materials overheating, oxidizing, and deteriorating as a result of direct irradiance from the concentrated sunlight and wear from the particles. New materials and operational strategies are being investigated to mitigate mesh deterioration.

Another obstructed flow design employs a spiral ramp along which particles flow under the influence of gravity and mechanically induced vibration (Xiao et al., 2014). Models and tests were performed that demonstrated that the particles could reach 650 °C at the outlet after 30 min of radiant power of 5 kW at the

Please cite this article in press as: Ho, C.K. Advances in central receivers for concentrating solar applications. Sol. Energy (2017), http://dx.doi.org/10.1016/j.solener.2017.03.048

Fig. 12. Images of particle flow over a staggered array of chevron-shaped mesh structures.

aperture. The measured thermal efficiency was ~60%. This design, however, requires beam-down optics, and a significant amount of particle flow may be challenging with this design.

Similar sliding particle receivers were investigated by Iniesta et al. (2015) in a beam-down receiver design. Particles were released into a conical ramp (funnel) and flowed down the ramp toward the center where the particles were collected in a bin beneath the opening. The particles were irradiated from above. The tests achieved ~600 °C with 2 kW of power and a particle flow rate of < 0.5 g/s.

3.1.3. Rotating kiln/centrifugal receivers

Rotating kilns were proposed as early as 1980 for use in solar particle heating applications (Flamant, 1982). The general principle is to feed particles into a rotating kiln/receiver with an aperture at one end of the receiver to allow incoming concentrated sunlight. The centrifugal force of the rotating receiver causes the particles to move along the walls of the receiver while they are irradiated by the concentrated sunlight. Early tests by Flamant et al. showed that these systems have a very high absorption factor (0.9–1), but the thermal efficiency was low (10–30%) for heating of $CaCo_3$ at particle mass flow rates of ~1 g/s. More recently, Wu et al. (2014a, 2014b, 2015a, 2015b) developed a centrifugal particle receiver design and prototype that employs a similar concept. Small bauxite ceramic particles (~1 mm) were introduced into a rotating centrifugal receiver with different inclination angles at mass flow rates of ~3–10 g/s. The particles were irradiated using a 15 kW_{th} solar simulator with an irradiance ranging from ~300 to 700 kW/m^2. For a face-down receiver inclination and incident irradiance of 670 kW/m^2, Wu et al. reported a particle outlet temperature of 900 °C and a receiver efficiency of about 75% (±4%) (Wu et al., 2015a). Challenges include maintaining a constant and sufficient mass flow rate of particles at larger scales, parasitic energy requirements, and reliability associated with a large rotating receiver system.

3.1.4. Fluidized particle receivers

Fluidization of solid particles in a solar receiver have been proposed for several decades, beginning in the late 1970s and early 1980s by Flamant et al. for thermochemical processing and heating (Flamant, 1982; Flamant et al., 1980) and by Sandia for power production (Falcone et al., 1985). Flamant (1982) and Flamant et al. (1980) tested a fluidized-bed receiver that consisted of a vertical transparent silica tube (15 cm long × 6.5 cm diameter) that was fluidized with compressed air from the bottom and irradiated at the top. Particles that were tested included zirconia, silica sand, chamotte, and silicon carbide. For a mean flux density of ~500 kW/m^2, the measured equilibrium temperature of the particles ranged from ~1200 K for silica sand to over 1400 K for silicon carbide particles. Thermal efficiencies were reported between 0.2 and 0.4 (Flamant et al., 1980). The ability to convey the particles and achieve adequate mass flow rates (for power production or continuous processes) may pose a challenge.

More recently, Benoit et al. (2015) and Flamant et al. (2014, 2013) have proposed and demonstrated an indirect particle receiver in which the particles are forced upward through irradiated tubes by airflow, which fluidizes the particles and increases heat transfer from the tube walls to the flowing particles. Particle temperature increases of greater than 200 °C were recorded in a 50 cm long stainless steel AISI 304L tube with irradiances ranging from ~200 to 400 W/m^2. Suspension temperatures at the outlet of the irradiated tubed were up to 750 °C, and the wall-to-suspension heat transfer coefficient was determined to be 420–1100 W/m^2-K for solid mass fluxes of 10–45 kg/m^2-s, respectively. Thermal efficiencies were not reported. Challenges in this system include parasitic energy requirements to fluidize the particles through the receiver tubes with sufficient mass flow to meet desired power requirements. The potential for hot spots and significant tube surface temperatures that radiate energy to the environment also exist.

Researchers at the Chinese Academy of Sciences (Bai et al., 2014; Wang et al., 2015; Zhang et al., 2015) have performed numerical and experimental studies on the thermal performance of an air receiver with silicon carbide particles in transparent quartz tubes. Air is blown upward through the particles in the quartz tubes while the tubes and particles are irradiated with concentrated sunlight from a 10 kW_{th} furnace. Results of those tests showed that the heated air reached over 600 °C with minimum temperature differences between the particles and the air below 10 °C, indicating good heat transfer between the air and the particles.

Steinfeld et al. (1992) designed and tested a fluidized bed receiver reactor that employed a vortical flow of air in a conical-shaped receiver. The particle/gas stream was introduced near the aperture, where concentrated sunlight entered the receiver and heated the swirling particles before the particles exited the receiver. The prototype reactor was tested to evaluate the thermal decomposition of calcium carbonate at 1300 K. The mean thermal absorption efficiency was 43% with a peak flux of ~1400 kW/m^2 at the aperture. Kodama et al. (2016, 2014) also investigated fluidized-bed receiver reactors with beam-down optics for water-splitting application. They achieved particle-bed temperatures over 1000 °C with 30 kW of applied power.

Another type of fluidized particle receiver involves the use of very small carbon particles dispersed in air that flows through the receiver. Concentrated sunlight irradiates and oxidizes the carbon particles, which volumetrically heats pressurized air passing through the receiver for high-temperature Brayton cycles. Abdelrahman et al. (1979) and Hunt (1979) first introduced this concept in 1979, and Hunt and Brown (1982) performed tests on a prototype receiver that heated the air to 1000 K. Miller and Koenigsdorff (Miller and Koenigsdorff, 1991; Miller and Koenigsdorff, 2000) developed theoretical analyses and thermal

modeling of the small particle solar receiver. Additional modeling and design optimization of the small particle heating receiver were performed in recent years as well (Crocker and Miller, 2012; del Campo et al., 2014; Fernandez and Miller, 2015; Kitzmiller and Miller, 2011). Potential advantages include the following: solar radiation is absorbed throughout the gas volume due to the large cumulative surface area of the particles; higher incident fluxes with no solid absorber that can be damaged; particles are oxidized leaving a particle free outlet stream (Miller and Koenigsdorff, 1991). Challenges include the development of a suitable window for the pressurized receiver and the development of a solid-gas suspension system that maintains a uniform particle concentration and temperature within the receiver.

3.1.5. Gravity-driven particle flow through enclosures

Ma and Zhang (2013), Ma et al. (2014), Martinek and Ma (2015) proposed an indirectly heated particle receiver with particles flowing downward under the force of gravity around a staggered array of tubes within an enclosure. The tubes were irradiated by concentrated sunlight on the interior surfaces while transferring heat to the particles flowing around the exterior side of the tubes inside of an enclosure (Fig. 13). Small-scale tests and models were performed that showed that the heat transfer to the particles was limited in locations around the tubular structures where the particles lost contact with the heated wall surfaces. Specific data on particle temperatures and thermal efficiencies were not available, and no on-sun tests have been performed. Other limitations may include maintaining a sufficient mass flow and obtaining a significant penetration and uniform flux of concentrated sunlight within the tubular cavities. Advantages to this design include no loss of particles through an open aperture and reduced heat losses relative to an open cavity receiver.

3.1.6. Summary of particle-based receivers

Table 2 summarizes the advantages and challenges of the particle-based receiver designs relative to one another. All particle receivers share the same advantages of a large operating temperature range with no freezing and no decomposition at temperatures well above 1000 °C, direct storage of the heat-transfer media, and the use of inert, relatively inexpensive particle media. Challenges shared by all particles receivers include the need for economical particle-to-working-fluid heat exchangers with high particle-side heat transfer coefficients, especially at high temperatures (>700 °C) and high pressures (>20 MPa), and mechanisms for high-temperature particle handling and flow control. Results from recent modeling and testing regarding outlet temperatures and thermal efficiencies are also presented.

3.2. High-temperature gas-based central receivers

Gas-based central receivers have been studied to provide heating for CSP applications using low- to high-pressure gases with or without storage (Heller et al., 2006; Hennecke et al., 2008; Zunft et al., 2011; Hoffschmidt et al., 2003; Lubkoll et al., 2015; Avila-Marin, 2011; Ho and Iverson, 2014; Karni et al., 1998; Ho et al., 2014; Liao et al., 2013; Atif et al., 2014). Advantages of gas-based receivers include the ability to achieve high temperatures (>1000 °C), use of inert and environmentally friendly gases, and low cost of the heat-transfer fluids. Challenges include low thermal conductivity and heat capacitance, flow instabilities, and the potential for costly equipment and materials if additional heat exchangers or high-temperature, high-pressure piping is required. Gas-based central receiver technologies include volumetric (open and closed; ambient and pressurized), tubular, and more recently, micro-channel configurations.

3.2.1. Volumetric air receivers

Volumetric air receivers employ porous structures (e.g., honeycombs, channels) that are irradiated by concentrated sunlight. Air flows through the irradiated porous structure and can be heated to temperatures between 800 and 1000 °C for metals, up to 1200 °C for ceramics, and up to 1500 °C for SiC (Avila-Marin, 2011). In theory, the air can be hottest in the interior of the receiver if the irradiance can penetrate deep into the porous receiver, but, in practice, the hottest portion of the volumetric receiver is at the aperture, where significant radiative losses occur. The hot air can be used to heat another working fluid (e.g., steam for a Rankine cycle) (Hennecke et al., 2008), charge a storage medium (Zunft et al., 2011), or pass directly into a gas turbine. Two reported applications of volumetric air receivers are (1) open-loop atmospheric volumetric air receivers for a Rankine cycle and (2) closed-loop pressurized (windowed) receivers for Brayton Cycles (Avila-Marin, 2011). Avila-Marin (2011) and Kribus et al. (1996) summarize a number of challenges associated with these designs, which include flow instabilities, large radiative losses, low thermal efficiencies, and structural limitations of pressurized quartz windows.

3.2.2. Tubular gas receivers

Tubular gas receivers for air-Brayton cycles have been evaluated for several decades (Heller et al., 2006; Bienert et al., 1979; Bechtel National Inc., 1981; Fan et al., 2007; Amsbeck et al., 2008; Amsbeck et al., 2009; Heller et al., 2009; Hischier et al., 2009; Amsbeck et al., 2010; Uhlig et al., 2011). Novel receiver designs employed liquid-metal heat pipes for parabolic dish receivers to improve exchange heat from the solar irradiance to the gas (Bienert et al., 1979). Other tubular central receiver designs and tests were conducted by DLR for a solarized microturbine system on the order of 100 kW – 1 MW (Heller et al., 2006; Amsbeck et al., 2008; Amsbeck et al., 2009; Heller et al., 2009; Amsbeck et al., 2010). New design concepts introduced in those studies include the use of absorber tubes with multiple layers consisting of Inconel and copper to enhance radial and circumferential heat transfer through the tube, segmented silica windows to reduce convective and radiative heat losses, and hybridization.

More recently, new tubular receiver configurations have been investigated to accommodate solarized supercritical CO_2 (sCO_2) Brayton cycles. Solarized sCO_2 Brayton cycles have been reported to theoretically achieve thermodynamic efficiencies approaching 50% and higher at concentration ratios and temperatures achievable by concentrating solar (Turchi et al., 2013; Ho et al., 2016d; Seidel, 2010; Angelino, 1968; Dostal et al., 2006). Pressures on the order of 15–25 MPa are expected for these sCO_2 Brayton cycles, making direct heating of pressurized sCO_2 challenging. Nevertheless, several studies describe the design of direct-sCO_2 tubular receiver that can accommodate high pressures (Ho et al., 2014; Liao et al., 2013; Atif et al., 2014; Besarati et al., 2015; Padilla et al., 2015; Gardner et al., 2016).

Bladed tubular receiver designs for sCO_2 and other gases have been investigated by several researchers as a means to increase light trapping and reduce convective and radiative losses (Bradshaw and Meeker, 1990; Christian et al., 2015; Christian et al., 2016; Ho et al., 2014; Bradshaw and Carling, 1987). Rather than using conventional cylindrical or cubical configurations for the receiver panels, researchers at Sandia National Laboratories, National Renewable Energy Laboratory, and Australian National University have proposed arranging the panels of tubes in radial or horizontal bladed configurations to enable reflected irradiance to be trapped rather than lost to the environment (Fig. 14). The cold fluid first flows to the leading edge of the blade and then serpentines back toward the interior of the receiver as it gets heated from the concentrated sunlight. Thus, the hottest part of the receiver is in the interior where the local radiative view factors (and

Please cite this article in press as: Ho, C.K. Advances in central receivers for concentrating solar applications. Sol. Energy (2017), http://dx.doi.org/10.1016/j.solener.2017.03.048

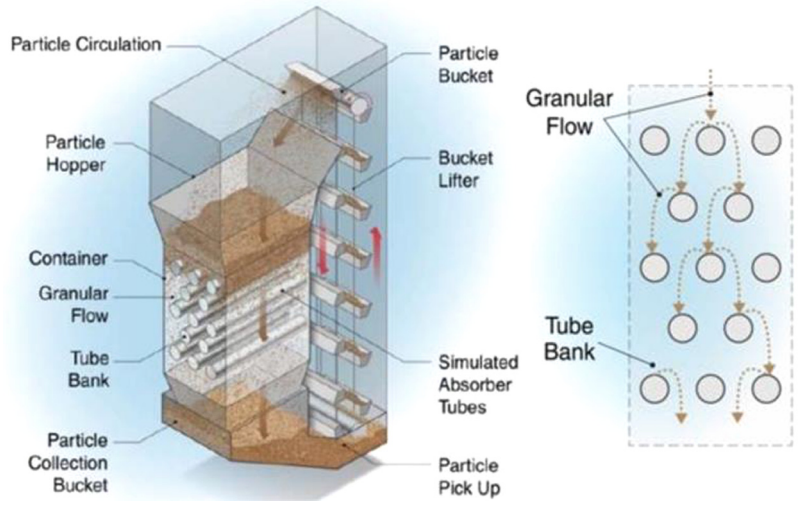

Fig. 13. Indirect particle receiver with particles flowing inside an enclosure around tubes whose interior surfaces are exposed to concentrated sunlight (Martinek and Ma, 2015).

Table 2
Summary of particle-based receiver designs.

Receiver design	Outlet temperature/ thermal efficiency	Advantages	Challenges/research needs	References
Free-falling direct absorption particle receiver	>700 °C/~90% (modeling of ~100 MW_e system), 50–80% (prototype testing ~1 MW_t)	Direct heating accommodates very large solar fluxes (~3000 sun); scalable to large capacities and particle mass flow rates	Increased convective heat losses from entrained airflow; particle loss through open aperture	Ho (2016), Ho et al. (2016a,c), Siegel et al. (2010), Gobereit et al. (2013), Christian and Ho (2014)
Obstructed-Flow Direct Absorption Particle Receiver	>800 °C/~60–90% (prototype testing ~1 MW_t)	Reduced velocity of particles (terminal velocity of ~0.5 m/s) resulting in increased residence time and heating; reduced entrainment of air flow and convective losses; potentially less particle loss	Potential overheating of obstruction materials with direct irradiance; additional cost of materials and complexity of installation	Ho (2016), Ho et al. (2016a, 2016c), Golob et al. (2016)
Centrifugal Direct Absorption Particle Receiver	~900 °C/~75% (prototype testing ~15 kW_t)	Controlled particle residence time based on rotational speed of receiver	Large rotating receiver; scalability to larger systems (~100 MW_t)	Wu et al., 2015a
Enclosed Falling Particle Receiver (Gravity Driven Flow)	>700 °C/~90% (modeling of enclosed receiver with aperture flux > ~1000 kW/m^2)	No particle loss and reduced convective loss	Large heat-transfer resistance between irradiated walls and particles; increased outer-wall surface temperature and potential for hot spots and limitations on solar flux	Martinek and Ma, 2015; Fleming et al., 2016
Enclosed Fluidized Particle Receiver	750 °C/Thermal efficiency to be determined	Increased particle-side heat transfer coefficient; no particle loss	Increased parasitics of fluidization; potential heat loss from fluidization gas; scalability of particle mass flow	Benoit et al., 2015; Flamant et al., 2014, 2013

heat loss) to the environment is lowest. Models of a horizontal bladed receiver configuration were developed and on-sun tests using compressed airflow through the bladed receiver panels were performed at Sandia National Laboratories (Ho et al., 2016e) (Fig. 14, right image). Test results showed that the thermal efficiency of the bladed receiver was up to ~6% greater than the flat receiver, and the effective solar absorptance (defined as the total absorbed irradiance divided by the incident irradiance striking the tubular surfaces) increased by up to 20% over the intrinsic solar absorptance due to light trapping effects. Previous studies have shown that convective losses can also be reduced through the disruption of thermal boundary layers and heat recuperation within the cavities of the bladed design. Challenges include structural requirements for the bladed configuration and ensuring that the leading edge of the blades do not overheat. (Ho et al., 2016e) painted the leading tubes of the horizontal blades white to avoid overheating and to match the absorbed surface flux over the majority of the receiver tubes).

Other methods have been investigated to increase light trapping and reduce heat losses from tubular receiver designs. Lubkoll et al. (2015) proposed a spiky central receiver air preheater (SCRAP) design that consists of a large number of spikes or tubes emanating from the receiver. Each spike consists of an inner and outer tube through which air flows; cold air flows through the inner tube toward the tip and then back along the outer tube. Similar to the bladed receiver design, the temperature of the outer surface of each tube is anticipated to rise from the spike tip to the interior root of each spike, where radiative losses are minimized. Simulations showed that radiative losses were only a few percent of the total incident power, but convective losses

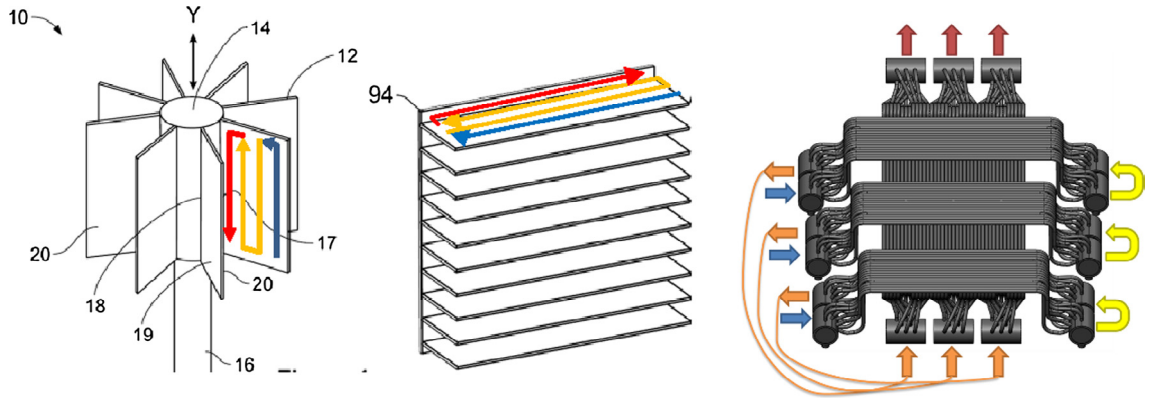

Fig. 14. Bladed receiver designs to enhance light trapping and reduce heat losses (Ho et al., 2016e; Ho et al., 2014).

were significantly higher (~16%) due to the large surface area. The thermal efficiency of a spike irradiated at 1 MW/m^2 with an air outlet temperature of ~800 °C was calculated at ~80%. Challenges include reducing the pressure drop within each spike and reducing convective losses.

Heller et al. (2016) evaluated a hybrid pressurized air receiver that consisted of a volumetric arrangement of tubes carrying high-pressure air that would be heated for a combined air-Brayton/steam-Rankine cycle. The volumetric arrangement of tubes was intended to allow penetration of the concentrated sunlight to interior portions of the receiver, exploiting the volumetric effect. A unique feature of their design was the additional use of a non-pressurized air stream that flowed around the tube array to preheat the air. However, simulations showed that the heating of external air flow by the tubes was insufficient to achieve desired temperatures. The authors recommend enhancements to improve heat transfer to the external flow and optical arrangement of the tube array.

Additional challenges with high-temperature tubular receivers include potentially large transient thermomechanical loads that can adversely affect the fatigue life of the receiver. Studies have been performed to understand the stresses and allowable flux limits on tubular receiver designs to optimize absorptance and thermal efficiency while mitigating the adverse effects of thermal stresses (Liao et al., 2013; Atif and Al-Sulaiman, 2014; Uhlig, 2011). Kolb compiled low-cycle fatigue data for Incoloy 800 HT, Inconel 625-LCF, and Haynes 230 alloys and performed analyses to determine allowable flux limits on these materials (Kolb, 2011). Additional materials considerations relevant to gas-phase central receivers are included in the section on liquid-based central receivers (Section 0).

3.2.3. Microchannel receivers

In recent years, researchers have investigated the use of microchannel receiver designs to increase the surface area between the gas heat-transfer fluid and the irradiated receiver walls (Padilla et al., 2015; Roldan and Fernandez-Reche, 2016; Ortega et al., 2016a; Ortega et al., 2016b). In this context, microchannel receivers refer to designs comprised of enclosed panels or plates with many small channels (as opposed to volumetric receivers with channels open to the environment). Brayton Energy has developed an internal finned-plate receiver design as part of the U.S. Department of Energy SunShot initiative that provides high heat transfer to the gas with structural integrity and tensile strength for high pressures (Fig. 15) Neber and Lee, 2013. They reported high receiver thermal efficiencies of 90% and long creep life (>90,000 h) and fatigue life (>100,000 cycles). Brayton Energy also introduced the concept of using an array of horizontal quartz tubes in front of the receiver panel to reduce radiative and convective losses (Neber and Lee, 2013).

Besarati et al. (2015) proposed a microchannel receiver based on compact heat exchanger technology. The receiver design consists of a group of plates with square-shaped channels diffusion bonded together to withstand high fluid pressures. Computational simulations showed that the receiver could heat sCO_2 with a mass flow rate of 1 kg/s from 530 °C to 700 °C with an irradiance of 500 kW/m^2. A parametric analysis was performed to optimize the receiver design by varying the hydraulic diameter, number of layers, and distance between the channels.

Oregon State University develop a microchannel receiver concept using an array of modular microchannel cells (L'Estrange et al., 2015; Rymal et al., 2014; Zada et al., 2016). The modular array consists of diffusion bonded parts with many short parallel microchannels, each having a hydraulic diameter on the order of hundreds of micrometers. An external central receiver would consist of an array of 1-m^2 panels with the array of microchannel cells. A reported advantage of the modular design is the ability to control the flow rates in each panel to accommodate varying flux levels while ensuring a prescribed outlet temperature. Modeling and testing showed that this receiver design (when applied to commercial scales) can achieve thermal efficiencies greater than 90% when heating sCO_2 to 650 °C with an irradiance of 1000 kW/m^2 (it should be noted that the definition of the thermal efficiency in that study neglected losses from reflected incident radiation and thermal losses that were ~15–20% of the total incident power to account for the small scale of the test cell (Roldan and Fernandez-Reche, 2016). This design produced two novel developments (1) the use of microchannels and an array of microscale pins for increased heat transfer from the walls to the fluid, and (2) the use of a branching fluidic distribution system to allow a large number of short microchannels operating in parallel to reduce pressure drop.

3.2.4. Storage considerations with gas receivers

Since direct storage of gases and supercritical fluids is not a viable option (Kelly, 2010), intermediate heat exchange with a separate storage media is required if thermals storage is desired with gas-based receivers. Solid and latent phase-change storage media have been proposed with gas receivers (Zunft et al., 2011; Ortega et al., 2016a; Nithyanandam and Pitchumani, 2013), but the cost and performance of these heat exchangers present additional challenges and need to be demonstrated.

3.2.5. Summary of gas-based receivers

Table 3 summarizes the advantages and challenges of the gas-based receiver designs. General advantages of gas-based receivers include the ability to achieve high temperatures (>1000 °C), use

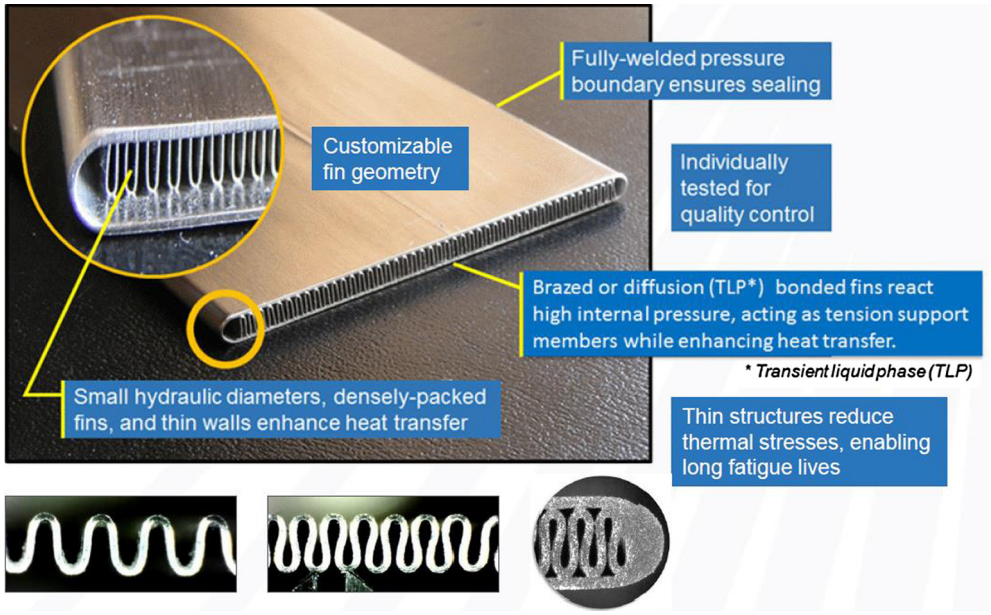

Fig. 15. Finned-plate receiver design with numerous mini-channels for fluid flow (Neber and Lee, 2013).

Table 3
Summary of gas-based receiver designs.

Receiver design	Outlet temperature/ thermal efficiency	Advantages	Challenges/research needs	References
Volumetric air receivers	>800 °C/50–90%	Use of ambient air (no cost), potential for volumetric (interior) heating to minimize heat losses near aperture	Flow instabilities, high temperatures and radiative heat losses near the aperture due to limited light penetration, no direct storage	Zunft et al., 2011; Avila-Marin, 2011; Kribus et al., 1996; Fend et al., 2013
Tubular gas receivers	700 – 800 °C / ~90% (modeling) Up to 85% (testing)	Ability to use features and geometry to increase light trapping	Heat-transfer resistance through tubes, fatigue, and high-cost materials to contain high-pressure, high-temperature flow, no direct storage	Heller et al., 2009; Amsbeck et al., 2010; Christian et al., 2015, 2016; Ortega et al., 2016a; Ho et al., 2016e; Neises et al., 2014; Ortega et al., 2016c; Ortega et al., 2016d
Microchannel gas receivers	~700 °C/Up to ~90% (scaled-up from bench-scale tests)	Increased surface area and heat transfer to gas, ability to "number-up" microchannel modules for larger capacities	Potential for increased pressure drop, potential manufacturing complexity and costs, no direct storage	Neber and Lee, 2013; L'Estrange et al., 2015; Rymal et al., 2014; Zada et al., 2016

of inert and environmentally friendly gases, and low cost of the heat-transfer fluids. Challenges include low thermal conductivity and heat capacitance, flow instabilities, and the potential for costly equipment and materials if additional heat exchangers or high-temperature, high-pressure piping is required.

3.3. High-temperature liquid-based central receivers

3.3.1. High-temperature molten salt

Current state-of-the-art molten salt receivers use a eutectic mixture of sodium and potassium nitrate (~60% $NaNO_3$, ~40% KNO_3). The freezing point of this "solar salt" is ~200 °C, and the upper operating temperature is limited to under ~600 °C due to decomposition (Bradshaw and Meeker, 1990) and corrosion of nickel alloys (Bradshaw and Goods, 2001). Nitrate salts are widely available as fertilizer and are inexpensive (~$1/kg) Ho et al., 2016f. In order to achieve higher operating temperatures above ~650 °C for advanced power cycles such as ultra-supercritical steam and sCO_2 Brayton cycles, halide and carbonate salt mixtures are being pursued.

3.3.1.1. Halide salts (Chlorides and Fluorides). Molten chloride salts have higher decomposition temperatures than molten nitrate salts, but they can be extremely corrosive to metals and alloys (Coyle et al., 1984; Gomez-Vidal and Tirawat, 2016; Mehos et al., 2017). Gomez-Vidal and Tirawat performed corrosion tests using a sodium and lithium chloride eutectic mixture (34.4 wt% NaCl, 65.6 wt% LiCl) at 650–700 °C in a nitrogen atmosphere and found that corrosion rates in various metals and nickel-based alloys were greater than ~3 mm/year, which was significantly greater than the desired corrosion rate of less than ~50 μm/year for CSP plants (Gomez-Vidal and Tirawat, 2016). Other chloride salt mixtures ($ZnCl_2$/NaCl/KCl and $MgCl_2$/KCl) have been proposed that have relatively low cost, good thermal stability at temperatures up to 750 °C, and potentially acceptable corrosion with affordable containment materials. Vignarooban et al. (2015) found that the corrosion rate of Hastelloy C-276 in a eutectic mixture of $ZnCl_2$/NaCl/KCl at 800 °C was only 10 μm/year in the absence of air. In the presence of air, the corrosion rate was found to be 500 μm/year at 800 °C. The magnesium-based chloride is less than half the cost of nitrate solar salt and can utilize corrosion mitigation via melt redox potential in inert atmospheres (Mehos et al., 2017).

However, magnesium-based chloride has the highest melting point and is extremely corrosive if oxygen or water is present. In addition, controlled purification and pre-melting procedures in inert atmospheres are required to remove impurities that may cause reactions and promote corrosion. The zinc-based chloride has the lowest melting point and also use corrosion mitigation via melt redox potential in inert atmospheres, but disadvantages include relative higher vapor pressure, extreme corrosivity in oxygen and water, relatively low heat capacity, and requirement of controlled purification and pre-melting procedures under vacuum (Mehos et al., 2017).

Fluoride salts have also been investigated for use in concentrating solar applications to increase operational temperatures up to 850 °C. Forsberg et al. (2007) propose using alkali fluorides, fluoroborates, or alkali-zirconium fluorides. They state that alkali fluorides like LiF-NaF-KF are very stable at high temperatures, nontoxic, and well understood. Fluoroborates are the lowest cost fluoride salt, but the headspace gas contains BF_3, which is reactive with water and forms corrosive compounds. Compared to chloride salts, Forsberg et al. (2007) state that the thermodynamic driving force for corrosion in fluoride salts is believed to be somewhat less than chlorides, although corrosion with fluoride salts is still a challenge. In addition, practical methods to purify fluorides have been developed, whereas purification methods for chloride salts have yet to be demonstrated.

3.3.1.2. Carbonate salts. Alkali carbonate salts are less corrosive than chloride or fluoride salts, and they do not require an inert headspace like the halide salts (Mehos et al., 2017). An et al. (2016) found that a ternary eutectic carbonate salt (Li2CO3-Na2CO3-K2CO3) can remain stable up to ~660 °C. Its high heat capacity and density reduces the required tank size, and ternary carbonate eutectics do not require highly controlled purification and pre-melting procedures like the chlorides. However, the carbonate salts have the highest cost and high melting points. In addition, the price of lithium may be impacted by markets that require lithium-ion batteries.

3.3.2. Liquid metals

Liquid sodium, lead-bismuth, and tin have been studied as possible heat-transfer fluids for central receiver systems operating at temperatures above 700 °C (Romero and González-Aguilar, 2017; Boerema et al., 2012; Coventry et al., 2015; Flesch et al., 2014; Kim et al., 2016; Lorenzin and Abanades, 2016; Pacio et al., 2014; Pacio and Wetzel, 2013). Liquid sodium has a very high thermal conductivity, which can allow higher solar fluxes on the receiver, greater receiver efficiencies, and lower thermal stresses on the tube walls (Ho and Iverson, 2014; Coventry et al., 2015). Sodium receivers employing liquid-vapor phase change through heat pipes and pool boilers have been tested for dish receivers, and their application to central receivers have been considered (Coventry et al., 2015). Sodium phase-change receivers may be good candidates for applications with isothermal heat sinks such as phase-change storage thermochemical processes. The cost of sodium (~$2/kg) is about twice has high as solar salt (~$0.7/kg - $1.5/kg) (Ho et al., 2016f; Lorenzin and Abanades, 2016).

Central receiver tests using liquid sodium were conducted in the 1980s at Sandia National Laboratories and Plataforma Solar de Almeria (PSA). The tests at Sandia consisted of a 3 m × 1.2 m sodium-cooled receiver panel designed and constructed by Rockwell International. Results showed that the receiver thermal efficiency exceeded 90% with irradiances up to ~1.5 MW/m^2, total power on the receiver of 1.85 MW_t, and sodium inlet/outlet temperatures of ~290 °C/590 °C (Rockwell International, 1983).

The sodium tests at PSA consisted of both cavity and external receiver designs (Romero and González-Aguilar, 2017; Coventry et al., 2015). The cavity receiver had a 9.7 m^2 aperture with a total absorbing area of 17 m^2. Results showed that the receiver thermal efficiency was less than expected, with calculated daily average efficiencies ranging from 67% to 76% at a total power of 2.8 MW_t, peak flux of 0.63 MW/m^2 inside the cavity, and sodium inlet/outlet temperatures of 270 °C/530 °C. The external receiver tested at PSA was a 7.9 m^2 billboard design and achieved daily average efficiencies up to 92% with a total power of 2.5 MW_t, peak flux of 1.4 MW/m^2, and sodium inlet/outlet temperatures of 270 °C/530 °C. Differences between the cavity and external receiver tests were attributed to higher convection losses and lower peak fluxes in the cavity receiver design.

In 2012, Vast Solar in Australia, commissioned a sodium receiver module consisting of a 2 m^2 flat tubular receiver panel on top of a 27 m tower at the Jemalong Solar Station. The receiver is irradiated by 700 heliostats to heat sodium from 270 °C to 560 °C with a total power of 1.2 MW_t and a peak flux of 1.5 MW/m^2 (Coventry et al., 2015). After successful testing of the single module, Vast Solar began construction of a 6 MW_{th} sodium power plant in 2014, consisting of five receiver modules and heliostat fields (Fig. 16). The plant will produce 1.1 MW_e with a steam turbine generator and have ~3 h of thermal storage using liquid sodium. The plant was expected to be commissioned in 2016, but a sodium leak in June of 2015 caused a fire that delayed commissioning (Romero and González-Aguilar, 2017). The fire prompted an evacuation of workers and neighbors, but the fire was extinguished without injury. After successful commissioning of the 6 MW_t sodium power plant, Vast Solar intends to construct a 30 MW_e utility-scale sodium power plant using the same modular design at Jemalong.

The primary drawback of sodium is its reactivity with water and flammability in air. As described above, a sodium leak caused significant delays for the Vast Solar pilot plant. At PSA, a significant sodium fire occurred in 1986 when 12 m^3 of sodium was ejected from pressurized storage tanks when maintenance was being performed (Romero and González-Aguilar, 2017; Coventry et al., 2015). Fortunately, no significant injuries occurred, but the plant was decommissioned. These incidents highlight the need for safe practices and training when using sodium.

Lead-bismuth has also been evaluated as a potential heat-transfer fluid for central receiver applications. It has a larger operating temperature range, with a boiling point of ~1600 °C vs. 880 °C. Lead-bismuth has a heat capacity that is nearly 40% larger than that of sodium and ~50% less than that of solar salt. Its thermal conductivity is about 4 times less than that of sodium and about 27 times that of solar salt. Lead-bismuth costs about 10–20 times more than solar salt ($13/kg vs. ~$0.7 - $1.5/kg), and it is very corrosive. In addition, corrosion and containment of lead-bismuth is a significant challenge. Kim et al. (2016) wrote that "Material availability for containing and transporting LBE (lead-bismuth eutectic) is the key issue before considering any application involving high temperature LBE alloy. There seems to be no proper metal-based material compatible with LBE for the temperature range of this study for a long term application."

Table 4 provides a summary of thermophysical properties for liquid sodium and liquid lead-bismuth metals relative to other heat-transfer media.

3.3.3. Tubular receiver materials

3.3.3.1. Nickel-based alloy receivers. Despite their higher costs relative to stainless steels, nickel-based alloys may be required for high-temperature receivers operating above 700 °C to maintain desired strength and corrosion resistance. Nickel-based alloys like Inconel 625 and Hastelloy C-276 were found to be the most corrosion-resistant to high-temperature salts relative to stainless steels (Gomez-Vidal and Tirawat, 2016; Vignarooban et al.,

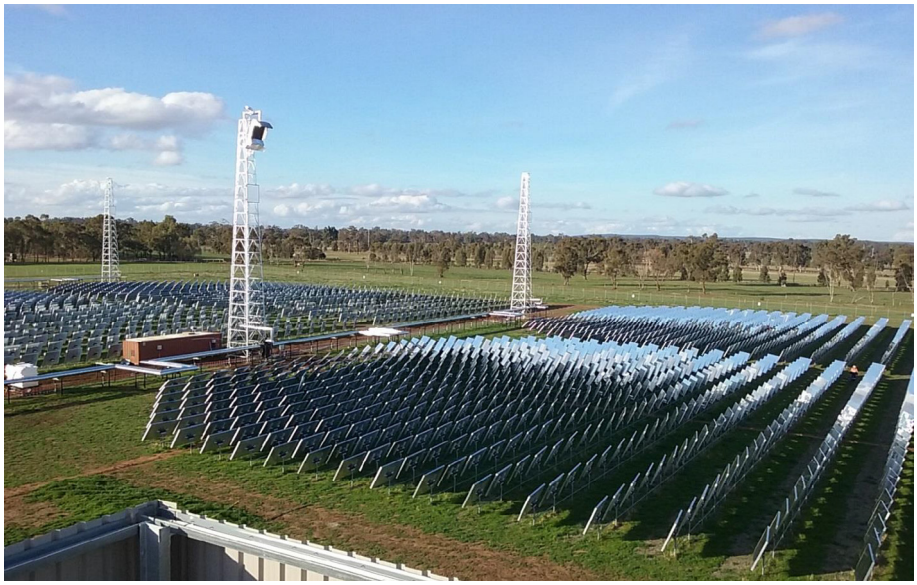

Fig. 16. Construction of the Vast Solar 6 MW_t sodium power plant at Jemalong Solar Station, Australia. Source: C.K. Ho, Sandia National Laboratories.

Table 4
Thermophysical properties of various heat transfer media at ~550 °C and 1 bar (Romero and González-Aguilar, 2017; Lorenzin and Abanades, 2016; Pacio et al., 2014; Incropera and DeWitt, 1985; Siegel et al., 2010).

Heat transfer media	k (W/m-K)	ρ (kg/m^3)	c_p (J/kg-K)
Solar salt	0.55	1800	1500
Liquid sodium	65	800	1300
Liquid lead-bismuth	15	10,000	140
Air	0.06	0.4	1100
Ceramic particles (direct heating)	2.0	2000	1200

2015). Haynes 230 has also been investigated and used for high-temperature solar receivers. Olivares et al. (2013) found that of the three nickel-based alloys (Haynes HR160, Hastelloy X, and Haynes 230) that they evaluated at temperatures up to 1050 °C, Haynes 230 showed the greatest resistance to oxidation in CO_2 and air. All three nickel-based alloys showed less corrosion in air than CO_2 due to the formation of a more protective oxide layer that formed in air.

3.3.3.2. Ceramic receivers. Silicon carbide is an attractive material for high-temperature solar receivers due to its high strength, high thermal conductivity, low thermal expansion, high solar absorptance, and chemical inertness at high temperatures. However, its brittleness can cause failure from mechanical shock. Ortona et al. (2015a, 2015b) describe the fabrication of SiC fiber-reinforced SiC matrix composites (SiC_f/SiC) for toughened high-temperature tubular receivers. The SiC_f/SiC tubes exhibit toughening as a result of "crack deflection, crack bridging, fiber pull-out and delamination mechanisms at the interface between the fibers and matrix". Test results of their SiC_f/SiC tube samples showed excellent heat transfer characteristics.

Sani et al. (2011, 2012) proposed ultra-high-temperature ceramics (hafnium and tantalum carbides) for use in high-temperature receiver applications. These carbides have melting temperatures above 3200 K, have good thermophysical properties, and are used in aerospace and high-temperature energy systems (turbine blades, combustors, nuclear reactors). Sani et al. (2011, 2012) measured the spectral emissivity of hafnium and tantalum carbides at temperatures between 1100 and 1500 K. Results show that the total hemispherical emissivity of the hafnium and tantalum carbides ranged from 0.2 to 0.6, which was considerably lower than the measured total hemispherical emissivity of silicon carbide (0.6 to 0.8). The solar absorptivity varied considerably, and was highest for hafnium carbide (up to 0.88) and lowest for dense tantalum carbides (0.4 to 0.5).

3.3.3.3. Solar selective coatings. Solar selective coatings exhibit high solar absorptance and low thermal emittance in the desired operating temperature range. The absorber efficiency, η_{abs}, is defined as the net radiative energy absorbed (absorbed incident solar radiation minus thermal radiative loss) divided by the total incident solar radiation:

$$\eta_{abs} = \frac{\alpha_s Q - \varepsilon\sigma T^4}{Q} = \alpha_s - \frac{\sigma T^4}{Q}\varepsilon \tag{3}$$

where α_s is the solar absorptivity, Q is the irradiance on the receiver (W/m^2), ε is the thermal emissivity, σ is the Stefan-Boltzmann constant (5.67×10^{-8} W/m^2/K^4), and T is the surface temperature (K). Eq. (3) shows that the relative importance (weighting) of the thermal emissivity to the solar absorptivity is given by the ratio of the thermal emission to the solar irradiance ($\sigma T^4/Q$). Fig. 17 plots this ratio as a function of temperature for different irradiance values. At a relatively low irradiance (concentration) value of 500 kW/m^2 (500 suns), the weighting of the thermal emissivity is only about 10% of that for solar absorptivity at a surface temperature of 700 °C. In other words, the solar absorptivity is an order of magnitude more important than the thermal emissivity in determining the net absorbed radiative energy at that temperature and irradiance. At higher irradiance values of 1000 kW/m^2 (1000 suns) and 1500 kW/m^2 (1500 suns), the relative importance of the thermal emissivity is even less for a given temperature. As the surface temperature increases, the relative importance of the thermal emissivity increases, but for practical receiver temperatures and irradiances, a high solar absorptance is more critical than a low thermal emissivity for efficient receivers.

Nevertheless, numerous studies have been performed to evaluate coatings and methods to develop selective absorbers with high solar absorptivity and low thermal emissivity (Ambrosini et al., 2011; Atkinson et al., 2015; Gray et al., 2015; Hall et al., 2012; Moon et al., 2015; Raccurt et al., 2015). Challenges include high costs, scalability of synthesis, and durability of these specialized

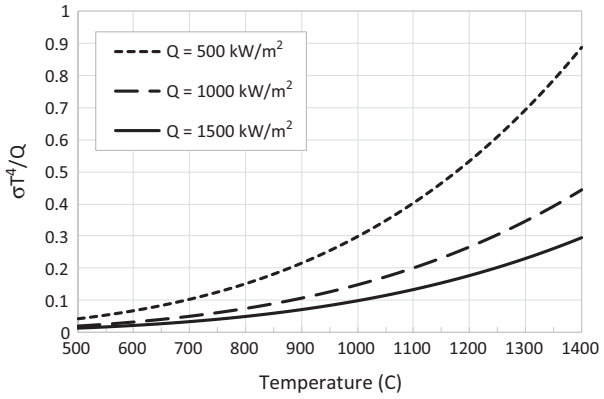

Fig. 17. Relative weighting of the thermal emissivity to solar absorptivity as a function of temperature and irradiance.

coatings at high temperatures in an oxidizing environment. Laser sintering, texturing, and the use of metamaterials to enhance solar absorptivity while reducing thermal emissivity have also been studied (Shah and Gupta, 2013; Shah et al., 2015; Wang et al., 2015). A commercial standard coating that has been used on central receivers for decades is high-temperature Pyromark 2500 paint (Ho et al., 2014). Although it is not a selective absorber, it has a very high solar absorptivity (~0.96), but it can degrade if not applied properly or when exposed to temperatures above ~700–800 °C over a period of time (Ho et al., 2012). In lieu of using coatings and textures, researchers have proposed the use of oxidized substrates (e.g., Haynes 230), which can yield solar absorptivities in excess of 90%, combined novel arrangement of tubular panels to increase the effective solar absorptance by several percentage points through light-trapping effects (Christian et al., 2016; Ho et al., 2014; Ortega et al., 2015).

3.3.4. Summary of liquid-based receivers

Table 5 summarizes the advantages and challenges of the liquid-based receiver designs.

4. Summary and conclusions

High-temperature central receivers are being pursed to increase the overall efficiency of concentrating solar power systems. Current state-of-the-art commercial central receiver systems employ steam or molten salt flowing through tubular panels. Peak outlet temperatures have been limited to less than ~600 °C due to heat-transfer limitations and stability of molten-nitrate salts. Higher temperature receivers are sought to enable higher efficiency power cycles operating at ~700 °C or higher. This paper provided a review of emerging particle, gas, and liquid-based receiver systems that can provide these higher temperatures.

Particle-based central receiver systems can operate over a very wide range of temperatures without the risk of freezing and decomposition. The particles are inert, inexpensive, and widely available. They include free-falling, obstructed, centrifugal, fluidized, and enclosed particle receiver designs. Directly irradiated particle systems have the advantage of allowing high peak fluxes that can increase the thermal efficiency, but challenges include particle loss and material handling at high temperatures. Enclosed particle receivers prevent particle loss, but additional heat-transfer resistance through the enclosure walls and possibly mass flow limitations pose challenges. Fluidization increases particle/wall heat transfer coefficients, but increases parasitics and potential heat losses associated with the fluidization. Challenges faced by all particles receivers include the need for economical particle-to-working-fluid heat exchangers with high particle-side heat transfer coefficients, and mechanisms for high-temperature particle handling and flow control.

Gas-based central receiver systems can achieve high temperatures (>1000 °C), but conventional volumetric air receivers have lacked high thermal efficiencies due to large radiative losses from the aperture. Also, the low thermal conductivity of gases limits the peak flux that can be applied in some configurations. New micro-channel designs have been proposed and tested to enable higher surface area and heat transfer, and results have shown the potential to achieve higher thermal efficiencies. Light-trapping configurations have also been studied and tested to increase the solar absorptance and reduce the effective thermal emittance of central receiver systems. A challenge with gas receiver systems is the need to utilize a separate storage medium such as solid or latent phase-change materials, and the associated heat exchangers. The cost and feasibility of these integrated storage and heat-exchanger systems with gas receivers at high temperatures remains to be demonstrated.

Current liquid-based receiver systems employ molten nitrate salts that decompose at ~600 °C. Halide salts (chlorides and fluorides) and carbonates that can reach temperatures in excess of 700 °C are being pursued, but corrosion and high cost need to be addressed. Liquid metals such as liquid sodium and liquid lead-bismuth eutetics have been studied to achieve higher temperatures. Liquid sodium has a very high thermal conductivity and can accommodate significantly higher fluxes for increased thermal efficiency. Demonstration plants using liquid sodium receivers

Table 5
Summary of liquid-based receiver designs.

Receiver design	Outlet temperature / thermal efficiency	Advantages	Challenges/research needs	References
Halide salt receiver	Up to ~800 °C / thermal efficiency to be determined	Ability to achieve high temperatures >700 °C, relatively low cost	Highly corrosive in the presence of air or water, requires controlled purification and pre-melting in a vaccum	Gomez-Vidal and Tirawat (2016), Mehos et al. (2017), Vignarooban et al. (2015), Forsberg et al. (2007)
Carbonate salt receiver	Up to ~800 °C/ thermal efficiency to be determined	Ability to achieve high temperatures ~700 °C, does not require controlled purification and pre-melting procedures	Very expensive	Mehos et al. (2017), An et al. (2016)
Liquid sodium receiver	530 °C (capable of up to ~800 °C)/ 90%	High thermal conductivity	Flammable in air, violent reactions with water	Romero and González-Aguilar (2017), Coventry et al. (2015), Benoit et al. (2016)
Lead-bismuth receiver	>~1000 °C/ Thermal efficiency to be determined	Very high boiling point, higher heat capacity than sodium but less than solar salt	Lower thermal conductivity than sodium, costs 10 – 20 times more than solar salt, very corrosive	Kim et al. (2016), Benoit et al. (2016)

Please cite this article in press as: Ho, C.K. Advances in central receivers for concentrating solar applications. Sol. Energy (2017), http://dx.doi.org/10.1016/j.solener.2017.03.048

have been built and tested for several decades, but safety and sodium fires are important issues that remain to be addressed. Lead-bismuth has good stability and a high boiling point, but it has lower thermal conductivity than sodium, is considerably more expensive, and is more corrosive.

Despite the challenges and competition faced by the concentrating solar power industry, central receivers have played an increased role in recently deployed CSP plants. The development of high-efficiency, high-temperature central receivers will be important to increase system performance, reduce levelized costs, and enable greater deployment of CSP plants around the world.

Acknowledgments

Sandia National Laboratories is a multi-mission laboratory managed and operated by Sandia Corporation, a wholly owned subsidiary of Lockheed Martin Corporation, for the U.S. Department of Energy's National Nuclear Security Administration under contract DE-AC04-94AL85000.

References

Abdelrahman, M., Fumeaux, P., Suter, P., 1979. Study of solid-gas-suspensions used for direct absorption of concentrated solar-radiation. Sol. Energy 22 (1), 45–48.

Ambrosini, A., Lambert, T.N., Bencomo, M., Hall, A., vanEvery, K., Siegel, N.P., Ho, C.K., 2011. Improved high temperature solar absorbers for use in concentrating solar power central receiver applications. In: Proceedings of the ASME 2011 Energy Sustainability and Fuel Cell Conference, ESFuelCell 2011–54241, Washington D. C., August 7–10, 2011.

Amsbeck, L., Buck, R., Heller, P., Jedamski, J., Uhlig, R., 2008. Development of a tube receiver for a solar-hybrid microturbine system. In: Proceedings of the 2008 SolarPACES Conference, Las Vegas, NV, March 4–7, 2008.

Amsbeck, L., Helsch, G., Roger, M., Uhlig, R., 2009. Development of a Broadband Antireflection Coated Transparent Silica Window for a Solar-Hybrid Microturbine Systems. In: Proceedings of SolarPACES 2009, Berlin, Germany, September 15–18, 2009.

Amsbeck, L., Denk, T., Ebert, M., Gertig, C., Heller, P., Herrmann, P., et al., 2010. Test of a solar-hybrid microturbine system and evaluation of storage deployment. In: Proceedings of SolarPACES 2010, Perpignan, France, September 21–24, 2010.

An, X.H., Cheng, J.H., Zhang, P., Tang, Z.F., Wang, J.Q., 2016. Determination and evaluation of the thermophysical properties of an alkali carbonate eutectic molten salt. Faraday Discuss. 190, 327–338.

Angelino, G., 1968. Carbon dioxide condensation cycles for power production. J. Eng. Power 90 (3), 287–296.

Atif, M., Al-Sulaiman, F.A., 2014. Performance analysis of supercritical CO_2 Brayton cycles integrated with solar central receiver system. In: 2014 5th International Renewable Energy Congress (Irec).

Atkinson, C., Sansom, C.L., Almond, H.J., Shaw, C.P., 2015. Coatings for concentrating solar systems - a review. Renew. Sustain. Energy Rev. 45, 113–122.

Avila-Marin, A.L., 2011. Volumetric receivers in solar thermal power plants with central receiver system technology: a review. Sol. Energy 85 (5), 891–910.

Bai, F., Zhang, Y., Zhang, X., Wang, F., Wang, Y., Wang, Z., 2014. Thermal performance of a quartz tube solid particle air receiver. In: Proceedings of the Solarpaces 2013 International Conference, vol. 49, pp. 284–294.

Bechtel National Inc., 1981, Preliminary Heat Pipe Testing Program: Final Technical Report, Contract No. DE-AC03-79SF 10756, San Francisco, CA.

Benoit, H., Lopez, I.P., Gauthier, D., Sans, J.L., Flamant, G., 2015. On-sun demonstration of a 750 degrees C heat transfer fluid for concentrating solar systems: dense particle suspension in tube. Sol. Energy 118, 622–633.

Benoit, H., Spreafico, L., Gauthier, D., Flamant, G., 2016. Review of heat transfer fluids in tube-receivers used in concentrating solar thermal systems: properties and heat transfer coefficients. Renew. Sustain. Energy Rev. 55, 298–315.

Besarati, S.M., Goswami, D.Y., Stefanakos, E.K., 2015. Development of a solar receiver based on compact heat exchanger technology for supercritical carbon dioxide power cycles. J. Solar Energy Eng.-Trans. ASME 137 (3).

Bienert, W.B., Rind, H., Wolf, A.A., 1979. Conceptual Design of an Open Cycle Air Brayton Solar Receiver: Phase 1 Final Report. DTM-79-1 Prepared under Contract No. 955135 for California Institute of Technology Jet Propulsion Laboratory, Dynatherm Corporation, Cockeysville, MD.

Boerema, N., Morrison, G., Taylor, R., Rosengarten, G., 2012. Liquid sodium versus Hitec as a heat transfer fluid in solar thermal central receiver systems. Sol. Energy 86 (9), 2293–2305.

Bradshaw, R.W., Carling, R.W., 1987. A review of the chemical and physical-properties of Molten alkali nitrate salts and their effect on materials for solar central receivers. J. Electrochem. Soc. 134 (8B), C510–C511.

Bradshaw, R.W., Goods, S.H., 2001. Accelerated Corrosion Testing of a Nickel-Base Alloy in a Molten Salt SAND2001-8758. Sandia National Laboratories, Albuquerque, NM.

Bradshaw, R.W., Meeker, D.E., 1990. High-temperature stability of ternary nitrate molten-salts for solar thermal-energy systems. Solar Energy Mater. 21 (1), 51–60.

Chen, H., Chen, Y., Hsieh, H.T., Siegel, N., 2007. CFD modeling of gas particle flow within a solid particle solar receiver. Proc. ASME Int. Solar Energy Conf., 37–48

Chen, Z.Q., Chen, Y.T., Tan, T.D., 2009. Numerical Analysis on the Performance of the Solid Solar Particle Receiver with the Influence of Aerowindow. In: Proceedings of the ASME Fluids Engineering Division Summer Conference -2008, vol. 1, Pt a and B, Jacksonville, FL.

Chirone, R., Salatino, P., Ammendola, P., Solimene, R., Magaldi, M., Sorrenti, R., Michele, G.D., Donatini, F., 2013, Development of a novel concept of solar receiver/thermal energy storage system based on compartmented dense gas fluidized beds. In: 14th International Conference on Fluidization - From Fundamentals to Products, Delft University of Technology, ECI Symposium Series.

Christian, J.M., Ho, C.K., 2013, Alternative designs of a high efficiency, north-facing, solid particle receiver. In: SolarPACES 2013, Las Vegas, NV, September 17–20, 2013.

Christian, J.M., Ho, C.K., 2014. System design of a 1 MW north-facing, solid particle receiver. In: Proceedings of the Solarpaces 2014 International Conference, Energy Procedia.

Christian, J., Ho, C., 2014. Alternative designs of a high efficiency, north-facing, solid particle receiver. In: Proceedings of the Solarpaces 2013 International Conference, vol. 49, pp. 314–323.

Christian, J.M., Ortega, J.D., Ho, C.K., 2015. Novel tubular receiver panel configurations for increased efficiency of high-temperature solar receivers. In: ASME Proceedings of the 9th International Conference on Energy Sustainability, San Diego, CA, June 28 - July 2, 2015.

Christian, J.M., Ortega, J.D., Ho, C.K., Yellowhair, J., 2016. Design and modeling of light-trapping tubular receiver panels. In: Proceedings of the ASME 2016 Power and Energy Conference, PowerEnergy2016-59158, Charlotte, North Carolina, June 26–30, 2016.

Coventry, J., Andraka, C., Pye, J., Blanco, M., Fisher, J., 2015. A review of sodium receiver technologies for central receiver solar power plants. Sol. Energy 122, 749–762.

Coyle, R.T., Burrows, R.W., Thomas, T.M., Lai, G.Y., 1984. Exploratory corrosion tests on alloys in Molten-salts at 900-Degrees-C. J. Metals 36 (7), p. 49-49.

Crocker, A., Miller, F., 2012. Coupled fluid flow and radiation modeling of a cylindrical small particle solar receiver. In: Proceedings of the Asme 6th International Conference on Energy Sustainability - 2012, Pts a and B, pp. 405–412.

del Campo, P.F., Miller, F., Crocker, A., 2014. Three-dimensional fluid dynamics and radiative heat transfer modeling of a small particle solar receiver. In: Proceedings of the ASME 7th International Conference on Energy Sustainability, 2013.

Dostal, V., Hejzlar, P., Driscoll, M.J., 2006. The supercritical carbon dioxide power cycle: comparison to other advanced power cycles. Nucl. Technol. 154 (Compendex), pp. 283–301.

Evans, G., Houf, W., Greif, R., Crowe, C., 1987. Gas-particle flow within a high-temperature solar cavity receiver including radiation heat-transfer. J. Solar Energy Eng.-Trans. ASME 109 (2), 134–142.

Falcone, P.K., 1986. A Handbook for Solar Central Receiver Design, SAND86-8009. Sandia National Laboratories, Livermore, CA.

Falcone, P.K., Noring, J.E., Hruby, J.M., 1985. Assessment of a Solid Particle Receiver for a High Temperature Solar Central Receiver System, SAND85-8208. Sandia National Laboratories, Livermore, CA.

Fan, Z.L., Zhang, Y.M., Liu, D.Y., Wang, J., Liu, W., 2007. Discussion of mechanical design for pressured cavity-air-receiver in solar power tower system. In: Proceedings of ISES Solar World Congress 2007: Solar Energy and Human Settlement, vols. I-V, pp. 1868–1872.

Fend, T., Schwarzbozl, P., Smirnova, O., Schollgen, D., Jakob, C., 2013. Numerical investigation of flow and heat transfer in a volumetric solar receiver. Renewable Energy 60, 655–661.

Fernandez, P., Miller, F.J., 2015. Performance analysis and preliminary design optimization of a Small Particle Heat Exchange Receiver for solar tower power plants. Sol. Energy 112, 458–468.

Flamant, G., 1982. Theoretical and experimental-study of radiant-heat transfer in a solar fluidized-bed receiver. AIChE J. 28 (4), 529–535.

Flamant, G., Hernandez, D., Bonet, C., Traverse, J.P., 1980. Experimental aspects of the thermochemical conversion of solar-energy - decarbonation of $CaCo_3$. Sol. Energy 24 (4), 385–395.

Flamant, G., Gauthier, D., Benoit, H., Sans, J.L., Garcia, R., Boissiere, B., Ansart, R., Hemati, M., 2013. Dense suspension of solid particles as a new heat transfer fluid for concentrated solar thermal plants: on-sun proof of concept. Chem. Eng. Sci. 102, 567–576.

Flamant, G., Gauthier, D., Benoit, H., Sans, J.L., Boissiere, B., Ansart, R., Hemati, M., 2014. A new heat transfer fluid for concentrating solar systems: particle flow in tubes. In: Proceedings of the Solarpaces 2013 International Conference, vol. 49, pp. 617–626.

Fleming, A., Ma, Z.W., Wendelin, T., Ban, H., Folsom, C., 2016. Thermal modeling of a multi-cavity array receiver performance for concentrating solar power generation. In: Proceedings of the ASME 9th International Conference on Energy Sustainability, 2015, vol. 1.

Flesch, J., Fritsch, A., Cammi, G., Marocco, L., Fellmoser, F., Pacio, J., Wetzel, T., 2014. 2015, Construction of a test facility for demonstration of a liquid lead-bismuth-cooled 10kW thermal receiver in a solar furnace arrangement - SOMMER. Int.

Conf. Concentrat. Solar Power Chem. Energy Syst., Solarpaces 2014 69, 1259–1268.
Forsberg, C.W., Peterson, P.F., Zhao, H.H., 2007. High-temperature liquid-fluoride-salt closed-Brayton-cycle solar power towers. J. Solar Energy Eng.-Trans ASME 129 (2), 141–146.
Gardner, W., Kim, J.S., McNaughton, R., Stein, W., Potter, D., 2016. Mechanical stress optimisation in a directly illuminated supercritical carbon dioxide solar receiver. In: Proceedings of the Asme Power Conference, 2016.
Gobereit, B., Amsbeck, L., Buck, R., Pitz-Paal, R., Müller-Steinhagen, H., 2012. Assessment of a Falling Solid Particle Receiver with Numerical Simulation, in SolarPACES 2012, Marrakech, Morrocco, September 11–14, 2012.
Gobereit, B., Amsbeck, L., Buck, R., 2013, Operation strategies for falling particle receivers. In: Proceedings of ASME 2013 7th International Conference on Energy Sustainability, ES-FuelCell 2013–18354, Minneapolis, MN, July 14–19, 2013.
Golob, M., Nguyen, C., Jeter, S.M., Abdel-Khalik, S., 2016. Solar simulator efficiency testing of lab-scale particle heating receiver at elevated operating temperatures. In: ASME 2016 10th International Conference on Energy Sustainability, ES2016-59619, Charlotte, NC, June 26–30, 2016.
Gomez-Vidal, J.C., Tirawat, R., 2016. Corrosion of alloys in a chloride molten salt (NaCl-LiCl) for solar thermal technologies. Sol. Energy Mater. Sol. Cells 157, 234–244.
Gray, M.H., Tirawat, R., Kessinger, K.A., Ndione, P.F., 2015. High temperature performance of high-efficiency, multi-layer solar selective coatings for tower applications. In: International Conference on Concentrating Solar Power and Chemical Energy Systems, Solarpaces 2014, vol. 69, pp. 398–404.
Hall, A., Ambrosini, A., Ho, C., 2012. Solar selective coatings for concentrating solar power central receivers. Adv. Mater. Processes 170 (1), 28–32.
Heller, P., Pfander, M., Denk, T., Tellez, F., Valverde, A., Fernandez, J., Ring, A., 2006. Test and evaluation of a solar powered gas turbine system. Sol. Energy 80 (10), 1225–1230.
Heller, L., Hoffmann, J., Gauche, P., 2016. The Hybrid Pressurized Air Receiver (HPAR) in the SUNDISC Cycle, Solarpaces 2015: International Conference on Concentrating Solar Power and Chemical Energy Systems, 1734.
Heller, P., Jedamski, J., Amsbeck, L., Uhlig, R., Ebert, M., Svensson, M., et al., 2009. Development of a solar-hybrid microturbine system for a mini-tower. In: Proceedings of SolarPACES 2009, Berlin, Germany, September 15–18, 2009.
Hennecke, K., Schwarzbozi, P., Alexopoulos, S., Gottsche, J., Hoffschmidt, B., Beuter, M., Koll, G., Hartz, T., 2008. Solar power tower Julich: the first test and demonstration plant for open volumetric receiver technology in Germany. In: SolarPACES, Las Vegas, NV, March 4–7, 2008.
Hischier, I., Hess, D., Lipinski, W., Modest, M., Steinfeld, A., 2009. Heat transfer analysis of a novel pressurized air receiver for concentrated solar power via combined cycles. In: Ht2009: Proceedings of the Asme Summer Heat Transfer Conference 2009, vol 1, pp. 105–112.
Ho, C.K., 2016. A review of high-temperature particle receivers for concentrating solar power. Appl. Therm. Eng. 109 (Part B), 958–969.
Ho, C.K., Christian, J.M., 2013. Evaluation of air recirculation for falling particle receivers. In Proceedings of ASME 2013 7th International Conference on Energy Sustainability, ES-FuelCell 2013–18236, Minneapolis, MN, July 14–19, 2013.
Ho, C.K., Iverson, B.D., 2014. Review of high-temperature central receiver designs for concentrating solar power. Renew. Sustain. Energy Rev. 29, 835–846.
Ho, C.K., Khalsa, S.S., Siegel, N.P., 2009. Modeling on-sun tests of a prototype solid particle receiver for concentrating solar power processes and storage. In: ES2009: Proceedings of the ASME 3rd International Conference on Energy Sustainability, vol. 2, San Francisco, CA.
Ho, C.K., Mahoney, A.R., Ambrosini, A., Bencomo, M., Hall, A., Lambert, T.N., 2012. Characterization of Pyromark 2500 for High-Temperature Solar Receivers. In: Proceedings of ASME 2012 6th International Conference on Energy Sustainability & 10th Fuel Cell Science, Engineering and Technology Conference, ESFuelCell 2012–91374, San Diego, CA, July 23–26, 2012.
Ho, C.K., Christian, J.M., Ortega, J.D., Yellowhair, J., Mosquera, M.J., Andraka, C.E., 2014. Reduction of radiative heat losses for solar thermal receivers. In: Proceedings of the SPIE Optics+Photonics Solar Energy+Technology High and Low Concentrator Systems for Solar Energy Applications IX, San Diego, August 17–21, 2014.
Ho, C.K., Christian, J.M., Pye, J., 2014. United States Patent Application 14535100, Bladed Solar Thermal Receivers for Concentrating Solar Power, Sandia Corporation, November 6, 2014.
Ho, C.K., Mahoney, A.R., Ambrosini, A., Bencomo, M., Hall, A., Lambert, T.N., 2014. Characterization of Pyromark 2500 paint for high-temperature solar receivers. J. Solar Energy Eng.-Trans. ASME 136 (1).
Ho, C.K., Conboy, T., Ortega, J., Afrin, S., Gray, A., Christian, J.M., Bandyopadyay, S., Kedare, S.B., Singh, S., Wani, P., 2014. High-temperature receiver designs for supercritical CO_2 closed-loop Brayton cycles. In: Proceedings of ASME 2014 8th International Conference on Energy Sustainability, ES-FuelCell 2014–6328, Boston, MA, June 29 - July 2, 2014.
Ho, C., Christian, J., Gill, D., Moya, A., Jeter, S., Abdel-Khalik, S., Sadowski, D., Siegel, N., Al-Ansary, H., Amsbeck, L., Gobereit, B., Buck, R., 2014, Technology advancements for next generation falling particle receivers. In: Proceedings of the Solarpaces 2013 International Conference, 49(Energy Procedia), pp. 398–407.
Ho, C.K., Christian, J.M., Moya, A.C., Taylor, J., Ray, D., Kelton, J., 2014. Experimental and numerical studies of air curtains for falling particle receivers. In: Proceedings of ASME 2014 8th International Conference on Energy Sustainability, ES-FuelCell 2014–6632, Minneapolis, MN, June 29 - July 2, 2014.
Ho, C.K., Christian, J., Romano, D., Yellowhair, J., Siegel, N., 2015. Characterization of particle flow in a free-falling solar particle receiver. In: Proceedings of the ASME 2015 Power and Energy Conversion Conference, San Diego, CA, June 28 - July 2, 2015.
Ho, C.K., Christian, J.M., Yellowhair, J., Siegel, N., Jeter, S., Golob, M., Abdel-Khalik, S. I., Nguyen, C., Al-Ansary, H., 2015. On sun testing of an advanced falling particle receiver system. In: SolarPACES 2015, Cape Town, South Africa, October 13–16, 2015.
Ho, C.K., Christian, J.M., Yellowhair, J., Siegel, N., Jeter, S., Golob, M., Abdel-Khalik, S. I., Nguyen, C., Al-Ansary, H., 2016a. On-sun testing of an advanced falling particle receiver system. Solarpaces 2015: International Conference on Concentrating Solar Power and Chemical Energy Systems 1734.
Ho, C.K., Mills, B., Christian, J.M., 2016b, Volumetric Particle Receivers for Increased Light Trapping and Heating. In: ASME Power & Energy Conference, Charlotte, NC, June 26–30, 2016
Ho, C.K., Christian, J.M., Yellowhair, J., Armijo, K., Jeter, S., 2016c. Performance evaluation of a high-temperature falling particle receiver. In: ASME Power & Energy Conference, Charlotte, NC, June 26–30, 2016.
Ho, C.K., Carlson, M., Garg, P., Kumar, P., 2016d. Technoeconomic analysis of alternative solarized s-CO_2 Brayton cycle configurations. J. Solar Energy Eng.-Trans. ASME 138 (5).
Ho, C.K., Ortega, J.D., Christian, J.M., Yellowhair, J.E., Ray, D., Kelton, J., Peacock, G., Andraka, C., 2016e. Fractal-Like Materials Design with Optimized Radiative Properties for High-Efficiency Solar Energy Conversion SAND2016-9526. Sandia National Laboratories, Albuquerque, NM.
Ho, C.K., Carlson, M., Garg, P., Kumar, P., 2016f. Technoeconomic analysis of alternative solarized s-CO_2 Brayton cycle configurations. J. Solar Energy Eng. 138, pp. 051008–1.
Ho, C.K., Christian, J.M., Yellowhair, J., Jeter, S., Golob, M., Nguyen, C., Repole, K., Abdel-Khalik, S.I., Siegel, N., Al-Ansary, H., El-Leathy, A., Gobereit, B., 2017. Highlights of the high-temperature falling particle receiver project: 2012–2016. In: SolarPaces 2016: international conference on concentrating solar power and chemical energy systems, Abu Dhabi, UAE, October 11–14, 2016.
Hoffschmidt, B., Tellez, F.M., Valverde, A., Fernandez, J., Fernandez, V., 2003. Performance evaluation of the 200-kW(th) HiTRec-II open volumetric air receiver. J. Solar Energy Eng.-Trans. ASME 125 (1), 87–94.
Hruby, J.M., 1986. A Technical Feasibility Study of a Solid Particle Solar Central Receiver for High Temperature Applications, SAND86-8211. Sandia National Laboratories, Livermore, CA.
Hruby, J.M., Steele, B.R., 1986. A solid particle central receiver for solar-energy. Chem. Eng. Prog. 82 (2), 44–47.
Hruby, J.M., Steele, B.R., Burolla, V.P., 1984. Solid Particle Receiver Experiments: Radiant Heat Test, Sandia National Laboratories SAND84-8251. Sandia National Laboratories, Albuquerque, NM.
Hunt, A.J., 1979. A new solar receiver utilizing a small particle heat exchanger. In: Proceedings of the 14th International Society of Energy Conversion Engineering Conference, Institute of Electrical and Electronics Engineers, New York.
Hunt, A.J., Brown, C.T., 1982. Solar testing of the small particle heat exchanger (SPHER), Lawrence Berkeley National Laboratory, Report no. LBL-16497, Berkeley, CA.
Incropera, F.P., DeWitt, D.P., 1985. Introduction to Heat Transfer. John Wiley & Sons, New York.
Iniesta, A.C., Diago, M., Delclos, T., Falcoz, Q., Shamim, T., Calvet, N., 2015. Gravity-fed combined solar receiver/storage system using sand particles as heat collector, heat transfer and thermal energy storage media. In: International Conference on Concentrating Solar Power and Chemical Energy Systems, Solarpaces 2014, vol. 69, pp. 802–811.
Karni, J., Kribus, A., Rubin, R., Doron, P., 1998. The "porcupine": a novel high-flux absorber for volumetric solar receivers. J. Solar Energy Eng.-Trans. ASME 120 (2), 85–95.
Kelly, B., 2010. Advanced Thermal Storage for Central Receivers With Supercritical Coolants, DE-FG36-08GO18149. Abengoa Solar Inc., Lakewood CO.
Khalsa, S.S.S., Ho, C.K., 2011. Radiation boundary conditions for computational fluid dynamics models of high-temperature cavity receivers. J. Solar Energy Eng.-Trans. ASME 133 (3).
Khalsa, S.S., Christian, J.M., Kolb, G.J., Roger, M., Amsbeck, L., Ho, C.K., Siegel, N.P., Moya, A.C., 2011, CFD Simulation and Performance Analysis of Alternative Designs for High-Temperature Solid Particle Receivers. In: Proceedings of the ASME 2011 Energy Sustainability and Fuel Cell Conference, ESFuelCell 2011–54430, Washington D.C., August 7–10, 2011.
Khayyat, A.W., Knott, R.C., Nguyen, C.L., Golob, M.C., Abdel-Khalik, S.I., Jeter, S.M., Al-Ansary, H.A., 2015. Measurement of particulate flow in discrete structure particle heating receivers. In: Proceedings of the ASME 2015 Power and Energy Conversion Conference, San Diego, CA, June 28 - July 2, 2015.
Kim, K., Moujaes, S.F., Kolb, G.J., 2010. Experimental and simulation study on wind affecting particle flow in a solar receiver. Sol. Energy 84 (2), 263–270.
Kim, J.S., Dawson, A., Wilson, R., Venkatesan, K., Stein, W., 2016. High-temperature heat transport and storage using LBE alloy for concentrated solar power system. In: Proceedings of the Asme 9th International Conference on Energy Sustainability, 2015, vol. 1.
Kitzmiller, K., Miller, F., 2011. Thermodynamic cycles for a small particle heat exchange receiver used in concentrating solar power plants. J. Solar Energy Eng.-Trans. ASME 133 (3).
Klein, H.H., Karni, J., Ben-Zvi, R., Bertocchi, R., 2007. Heat transfer in a directly irradiated solar receiver/reactor for solid-gas reactions. Sol. Energy 81 (10), 1227–1239.

Please cite this article in press as: Ho, C.K. Advances in central receivers for concentrating solar applications. Sol. Energy (2017), http://dx.doi.org/10.1016/j.solener.2017.03.048

Knott, R., Sadowski, D.L., Jeter, S.M., Abdel-Khalik, S.I., Al-Ansary, H.A., El-Leathy, A., 2014, High temperature durability of solid particles for use in particle heating concentrator solar power systems. In: Proceedings of the ASME 2014 8th International Conference on Energy Sustainability, ES-FuelCell 2014–6586, Boston, MA, June 29 - July 2, 2014.

Kodama, T., Gokon, N., Matsubara, K., Yoshida, K., Koikari, S., Nagase, Y., Nakamura, K., 2014. Flux measurement of a new beam-down solar concentrating system in Miyazaki for demonstration of thermochemical water splitting reactors. In: Proceedings of the Solarpaces 2013 International Conference, vol. 49, pp. 1990–1998.

Kodama, T., Gokon, N., Cho, H.S., Matsubara, K., Etori, T., Takeuchi, A., Yokota, S., Ito, S., 2016. Particles fluidized bed receiver/reactor with a beam-down solar concentrating optics: 30-kW(th) performance test using a big sun-simulator. In: Solarpaces 2015: International Conference on Concentrating Solar Power and Chemical Energy Systems, 1734.

Kolb, G.J., 2011. An Evaluation of Possible Next-Generation High-Temperature Molten-Salt Power Towers SAND2011-9320. Sandia National Laboratories, Albuquerque, NM.

Kolb, G.J., United States Patent U.S. Patent# 8,109,265, 12/368,327, Suction-Recirculation Device for Stabilizing Particle Flows Within a Solar Powered Solid Particle Receiver, Sandia National Laboratories, February 7, 2012.

Kolb, G.J., Diver, R.B., Siegel, N., 2007. Central-station solar hydrogen power plant. J. Solar Energy Eng.-Trans. ASME 129 (2), 179–183.

Kribus, A., Ries, H., Spirkl, W., 1996. Inherent limitations of volumetric solar receivers. J. Solar Energy Eng.-Trans. ASME 118 (3), 151–155.

Lee, T., Lim, S., Shin, S., Sadowski, D.L., Abdel-Khalik, S.I., Jeter, S.M., Al-Ansary, H., 2015. Numerical simulation of particulate flow in interconnected porous media for central particle-heating receiver applications. Sol. Energy 113, 14–24.

L'Estrange, T., Truong, E., Rymal, C., Rasouli, E., Narayanan, V., Apte, S., Drost, K., 2015. High flux microscale solar thermal receiver for supercritical carbon dioxide cycles. In: Proceedings of the Asme 13th International Conference on Nanochannels, Microchannels, and Minichannels, 2015.

Liao, B., Guo, L.J., Lu, Y.J., Zhang, X.M., 2013. Solar receiver/reactor for hydrogen production with biomass gasification in supercritical water. Int. J. Hydrogen Energy 38 (29), 13038–13044.

Lorenzin, N., Abanades, A., 2016. A review on the application of liquid metals as heat transfer fluid in Concentrated Solar Power technologies. Int. J. Hydrogen Energy 41 (17), 6990–6995.

Lubkoll, M., von Backstrom, T.W., Harms, T.M., Kroger, D.G., 2015. Initial analysis on the novel Spiky Central Receiver Air Pre-heater (SCRAP) pressurized air receiver. International Conference on Concentrating Solar Power and Chemical Energy Systems, Solarpaces 2014 69, 461–470.

Ma, Z., Zhang, R., 2013. United States Patent 13/855,092, Solid Particle Thermal Energy Storage Design for a Fluidized-Bed Concentrating Solar Power Plant, NREL, April 2, 2013.

Ma, Z.W., Glatzmaier, G., Mehos, M., 2014. Fluidized bed technology for concentrating solar power with thermal energy storage. J. Solar Energy Eng.-Trans. ASME 136 (3).

Martin, J., John Vitko, J., 1982. ASCUAS: A Solar Central Receiver Utilizing a Solid Thermal Carrier, Sandia National Laboratories SAND82-8203. Sandia National Laboratories, Livermore, CA.

Martinek, J., Ma, Z., 2015. Granular flow and heat-transfer study in a near-blackbody enclosed particle receiver. J. Sol.Energy Eng. 137 (5), p. 051008-051008.

Mehos, M., Turchi, C., Jorgensen, G., Denholm, P., Ho, C.K., Armijo, K., 2016. On the Path to SunShot: Advancing Concentrating Solar Power Technology, Performance, and Dispatchability, NREL/TP-5500-65688. National Renewable Energy Laboratory, Golden, CO. <http://www.nrel.gov/docs/fy16osti/65688.pdf>.

Mehos, M., Turchi, C., Vidal, J., Wagner, M., Ma, Z., Ho, C., Kolb, W., Andraka, C., Kruizenga, A., 2017. Concentrating Solar Power Gen3 Demonstration Roadmap NREL/TP-5500-67464. National Renewable Energy Laboratory, Golden, CO.

Meier, A., 1999. A predictive CFD model for a falling particle receiver reactor exposed to concentrated sunlight. Chem. Eng. Sci. 54 (13–14), 2899–2905.

Miller, F., Koenigsdorff, R., 1991. Theoretical-analysis of a high-temperature small-particle solar receiver. Solar Energy Mater. 24 (1–4), 210–221.

Miller, F.J., Koenigsdorff, R.W., 2000. Thermal modeling of a small-particle solar central receiver. J. Solar Energy Eng.-Trans. ASME 122 (1), 23–29.

Moon, J., Kim, T.K., VanSaders, B., Choi, C., Liu, Z.W., Jin, S.H., Chen, R.K., 2015. Black oxide nanoparticles as durable solar absorbing material for high-temperature concentrating solar power system. Sol. Energy Mater. Sol. Cells 134, 417–424.

Neber, M., Lee, H., 2013. Silicon carbide solar receiver for residential scale concentrated solar power. Int. Mech. Eng. Cong. Expos. - 2012 Vol 6 Pts a and B, 371–376.

Neises, T.W., Wagner, M.J., Gray, A.K., 2014. Structural design considerations for tubular power tower receivers operating at 650 Degrees C. In: Proceedings of the ASME 8th International Conference on Energy Sustainability, 2014, vol. 1.

Nithyanandam, K., Pitchumani, R., 2013. Computational studies on a latent thermal energy storage system with integral heat pipes for concentrating solar power. Appl. Energy 103, 400–415.

Olivares, R.I., Stein, W., Marvig, P., 2013. Thermogravimetric study of oxidation-resistant alloys for high-temperature solar receivers. JOM 65 (12), 1660–1669.

Ortega, J.D., Christian, J.M., Ho, C.K., 2015. Coupled optical-thermal-fluid and structural analyses of novel light-trapping tubular panels for concentrating solar power receivers. In: Proceedings of the SPIE Optics+Photonics Solar Energy +Technology High and Low Concentrator Systems for Solar Energy Applications X, San Diego, August 9–13, 2015.

Ortega, J.D., Christian, J.M., Ho, C.K., 2016. Structural analysis of a direct heated tubular solar receiver for supercritical CO_2 Brayton cycle. In: Proceedings of the ASME 9th International Conference on Energy Sustainability, 2015, vol. 1.

Ortega, J.D., Khivsara, S.D., Christian, J.M., Yellowhair, J.E., Ho, C.K., 2016. Coupled optical-thermal-fluid modeling of a directly heated tubular solar receiver for supercritical CO_2 Brayton cycle. In: Proceedings of the Asme 9th International Conference on Energy Sustainability, 2015, vol. 1.

Ortega, J., Khivsara, S., Christian, J., Ho, C., Dutta, P., 2016c. Coupled modeling of a directly heated tubular solar receiver for supercritical carbon dioxide Brayton cycle: structural and creep-fatigue evaluation. Appl. Therm. Eng. 109, 979–987.

Ortega, J., Khivsara, S., Christian, J., Ho, C., Yellowhair, J., Dutta, P., 2016d. Coupled modeling of a directly heated tubular solar receiver for supercritical carbon dioxide Brayton cycle: optical and thermal-fluid evaluation. Appl. Therm. Eng. 109, 970–978.

Ortona, A., Fend, T., Yu, H.W., Raju, K., Fitriani, P., Yoon, D.H., 2015a. Tubular Si-infiltrated SiCf/SiC composites for solar receiver application-Part 1: Fabrication by replica and electrophoretic deposition. Sol. Energy Mater. Sol. Cells 132, 123–130.

Ortona, A., Yoon, D.H., Fend, T., Feckler, G., Smirnova, O., 2015b. Tubular Si-infiltrated SiCf/SiC composites for solar receiver application - Part 2: Thermal performance analysis and prediction. Sol. Energy Mater. Sol. Cells 140, 382–387.

Pacio, J., Wetzel, T., 2013. Assessment of liquid metal technology status and research paths for their use as efficient heat transfer fluids in solar central receiver systems. Sol. Energy 93, 11–22.

Pacio, J., Fritsch, A., Singer, C., Uhlig, R., 2014. Liquid metals as efficient coolants for high-intensity point-focus receivers: implications to the design and performance of next-generation CSP systems. In: Proceedings of the Solarpaces 2013 International Conference, vol. 49, pp. 647–655.

Padilla, R.V., Too, Y.C.S., Beath, A., McNaughton, R., Stein, W., 2015. Effect of pressure drop and reheating on thermal and exergetic performance of supercritical carbon dioxide Brayton cycles integrated with a solar central receiver. J. Solar Energy Eng.-Trans. ASME 137 (5).

Raccurt, O., Disdier, A., Bourdon, D., Donnola, S., Stollo, A., Gioconia, A., 2015. Study of the stability of a selective solar absorber coating under air and high temperature conditions. In: International Conference on Concentrating Solar Power and Chemical Energy Systems, Solarpaces 2014, vol. 69, pp. 1551–1557.

Rockwell International, 1983. Final Report Sodium Solar Receiver Experiment, SAND82-8192, Sandia National Laboratories, December 1983.

Röger, M., Amsbeck, L., Gobereit, B., Buck, R., 2011. Face-down solid particle receiver using recirculation. J. Solar Energy Eng.-Trans. ASME 133, 3.

Roldan, M.I., Fernandez-Reche, J., 2016. CFD analysis of supercritical CO_2 used as HTF in a solar tower receiver. In: Solarpaces 2015: International Conference on Concentrating Solar Power and Chemical Energy Systems, 1734.

Romero, M., González-Aguilar, J., 2017. 7 - Next Generation of Liquid Metal and Other High-Performance Receiver Designs for Concentrating Solar Thermal (CST) Central Tower Systems A2 - Blanco, Manuel J, Advances in Concentrating Solar Thermal Research and Technology. Woodhead Publishing, L.R. Santigosa.

Rymal, C.J., Apte, S.V., Narayanan, V., Drost, K., 2014. Numerical design of a planar high-flux microchannel solar receiver. In: Proceedings of the Asme 8th International Conference on Energy Sustainability, 2014, vol. 1.

Röger, M., Amsbeck, L., Gobereit, B., Buck, R., 2011. Face-down solid particle receiver using recirculation. J. Sol.Energy Eng.

Sani, E., Mercatelli, L., Fontani, D., Sans, J.L., Sciti, D., 2011. Hafnium and tantalum carbides for high temperature solar receivers. J. Renew. Sustain. Energy 3 (6).

Sani, E., Mercatelli, L., Sansoni, P., Silvestroni, L., Sciti, D., 2012. Spectrally selective ultra-high temperature ceramic absorbers for high-temperature solar plants. J. Renew. Sustain. Energy 4 (3).

Seidel, W., 2010. Model development and annual simulation of the supercritical carbon dioxide Brayton cycle for concentrating solar power applications. In: Mechanical Engineering 2010, University of Wisconsin-Madison.

Shah, A.A., Gupta, M.C., 2013. Spectral selective surfaces for concentrated solar power receivers by laser sintering of tungsten micro and nano particles. Sol. Energy Mater. Sol. Cells 117, 489–493.

Shah, A.A., Ungaro, C., Gupta, M.C., 2015. High temperature spectral selective coatings for solar thermal systems by laser sintering. Sol. Energy Mater. Sol. Cells 134, 209–214.

Siegel, N.P., Ho, C.K., Khalsa, S.S., Kolb, G.J., 2010. Development and evaluation of a prototype solid particle receiver: on-sun testing and model validation. J. Solar Energy Eng.-Trans. ASME 132 (2).

Siegel, N., Gross, M., Ho, C., Phan, T., Yuan, J., 2014. Physical properties of solid particle thermal energy storage media for concentrating solar power applications. In: Proceedings of the Solarpaces 2013 International Conference, 49(Energy Procedia), pp. 1015–1023.

Siegel, N.P., Gross, M.D., Coury, R., 2015. The development of direct absorption and storage media for falling particle solar central receivers. ASME J. Solar Energy Eng. 137 (4), p. 041003–041003-7.

Steinfeld, A., Imhof, A., Mischler, D., 1992. Experimental investigation of an atmospheric-open cyclone solar reactor for solid-gas thermochemical reactions. J. Solar Energy Eng.-Trans. ASME 114 (3), 171–174.

Tan, T.D., Chen, Y.T., 2009. Protection of an Aerowindow, One Scheme to Enhance the Cavity Efficiency of a Solid Particle Solar Receiver. In: HT2009: Proceedings of the ASME Summer Heat Transfer Conference 2009, vol. 2, San Francisco, CA.

Tan, T.D., Chen, Y.T., 2010. Review of study on solid particle solar receivers. Renew. Sustain. Energy Rev. 14 (1), 265–276.

Please cite this article in press as: Ho, C.K. Advances in central receivers for concentrating solar applications. Sol. Energy (2017), http://dx.doi.org/10.1016/j.solener.2017.03.048

Tan, T.D., Chen, Y.T., Chen, Z.Q., Siegel, N., Kolb, G.J., 2009. Wind effect on the performance of solid particle solar receivers with and without the protection of an aerowindow. Sol. Energy 83 (10), 1815–1827.

Turchi, C.S., Ma, Z.W., Neises, T.W., Wagner, M.J., 2013. Thermodynamic study of advanced supercritical carbon dioxide power cycles for concentrating solar power systems. J. Solar Energy Eng.-Trans. ASME 135 (4).

Uhlig, R., 2011, Transient Stresses at Metallic Solar Tube Receivers, in Proceedings of SolarPACES 2011, Granada, Spain, September 20–23, 2011.

Vignarooban, K., Xu, X.H., Wang, K., Molina, E.E., Li, P., Gervasio, D., Kannan, A.M., 2015. Vapor pressure and corrosivity of ternary metal-chloride molten-salt based heat transfer fluids for use in concentrating solar power systems. Appl. Energy 159, 206–213.

Wang, H., Sivan, V.P., Mitchell, A., Rosengarten, G., Phelan, P., Wang, L.P., 2015. Highly efficient selective metamaterial absorber for high-temperature solar thermal energy harvesting. Sol. Energy Mater. Sol. Cells 137, 235–242.

Wang, F., Bai, F., Wang, Z., Zhang, X., 2015. Numerical simulation of quartz tube solid particle air receiver. In: International Conference on Concentrating Solar Power and Chemical Energy Systems, Solarpaces 2014, vol. 69, pp. 573–582.

Wu, W., Amsbeck, L., Buck, R., Uhlig, R., Ritz-Paal, R., 2014. Proof of concept test of a centrifugal particle receiver, Proceedings of the Solarpaces 2013 International Conference, vol. 49, pp. 560–568.

Wu, W., Amsbeck, L., Buck, R., Waibel, N., Langner, P., Pitz-Paal, R., 2014b. On the influence of rotation on thermal convection in a rotating cavity for solar receiver applications. Appl. Therm. Eng. 70 (1), 694–704.

Wu, W., Trebing, D., Amsbeck, L., Buck, R., Pitz-Paal, R., 2015a. Prototype testing of a centrifugal particle receiver for high-temperature concentrating solar applications. J. Solar Energy Eng.-Trans. ASME 137 (4).

Wu, W., Uhlig, R., Buck, R., Pitz-Paal, R., 2015b. Numerical simulation of a centrifugal particle receiver for high-temperature concentrating solar applications. Numer. Heat Transf. A-Applicat. 68 (2), 133–149.

Xiao, G., Guo, K.K., Ni, M.J., Luo, Z.Y., Cen, K.F., 2014. Optical and thermal performance of a high-temperature spiral solar particle receiver. Sol. Energy 109, 200–213.

Zada, K.R., Hyder, M.B., Drost, M.K., Fronk, B.M., 2016. Numbering-up of microscale devices for megawatt-scale supercritical carbon dioxide concentrating solar power receivers. J. Solar Energy Eng.-Trans. ASME 138 (6).

Zhang, Y.N., Bai, F.W., Zhang, X.L., Wang, F.Z., Wang, Z.F., 2015. Experimental study of a single quartz tube solid particle air receiver. In: International Conference on Concentrating Solar Power and Chemical Energy Systems, Solarpaces 2014, vol. 69, pp. 600–607.

Zunft, S., Hanel, M., Kruger, M., Dreissigacker, V., Gohring, F., Wahl, E., 2011. Julich solar power tower-experimental evaluation of the storage subsystem and performance calculation. J. Solar Energy Eng.-Trans. ASME 133 (3).

Please cite this article in press as: Ho, C.K. Advances in central receivers for concentrating solar applications. Sol. Energy (2017), http://dx.doi.org/10.1016/j.solener.2017.03.048